Chapter VI

Characterization of Gas Sensors

In the previous chapter, the preparation of tin alkoxide precursor and the fabrication processes of thin film gas sensors were discussed. In this chapter, the characterizations of gas sensors such as I-V characteristic, gas response characteristics will be described.

In this work, gas sensors had been fabricated from three different precursors.

- the commercial sol solution
- the sol solution synthesized by the sodium method with the simple mixed processes (section 5.2.3)
- the sol solution synthesized by the sodium method with the rigorously controlled processes (section 5.2.4)

The characterizations of gas response were performed by using the gas measuring system described in chapter III and, our proposed measuring circuit in chapter IV. Table 6.1 shows the condition using in the characterization of gas response.

Table 6.1 Conditions for characterization of gas sensing performance.

Parameters	Conditions
V_{in}	5 V
Operating temperature	150 - 400 °C
Flow rate of carrier gas	400 ml/min (O_2 80 ml/min and N_2 320 ml/min)
Test sample	methyl alcohol 0.01 - 10 % by volume
	ammonia 0.01 - 10 % by volume
Injection volume	6 μl

6.1 Power Law Model

To analyze the gas sensing performance in more quantitative details, Clifford and Tuma[57] has adopted the power law relationship. The power law can be expressed as follows.

$$R = R_o(1 + k \cdot [C])^{-\beta} \tag{6.1}$$

In this expression, R represents the measured resistance value of gas sensor in the concentration of reducing gas: $[C]$. R_o is the resistance under zero concentration of gas, β is the dimensionless power law exponent and k is the constant of dimension of $[C]^{-1}$. In general case, we can expand Eq. (6.1) to get the expression of sensitivity as shown in Eq. (6.2)

$$S = \frac{R_o}{R} = (1 + k \cdot [C])^{\beta} \tag{6.2}$$

This expression is suitable for the case where the gas sample is calibrated or standardized with synthetic air (Fig. 6.1(a)). This condition does not match with our experiments, in which the test samples are prepared by dilution with de-ionized water (DI). This means that all gas concentrations are described in the term of percents by volume in water. Therefore, in our experiments, the response to the zero concentration of a test sample refers to the response to the DI water. This is shown schematically in Fig. 6.1(b). With the above reason, Eq. (6.2) can not be fitted very well with our experimental results. Therefore, a modified power law which is more suitable to the experimental data, has been proposed. The modified power law is expressed in the follow.

$$S = a \cdot (1 + k \cdot [C])^{\beta} \tag{6.3}$$

The additional term, a refers to the sensitivity of gas sensor to pure water. The parameters in Eq. (6.3) can be used to compared the performance of gas sensing quantitatively. For example, k can be used to indicate the threshold of detection of the concentration of a test sample at which the calibration curve changes its slope

from the horizontal line. This occurs when $[C] = 1/k$. Above the threshold, we can observe the change of sensitivity with gas concentration. In the log-log plot, β determines the slope of the calibration curve or the rate of change of sensitivity with the sample concentration.

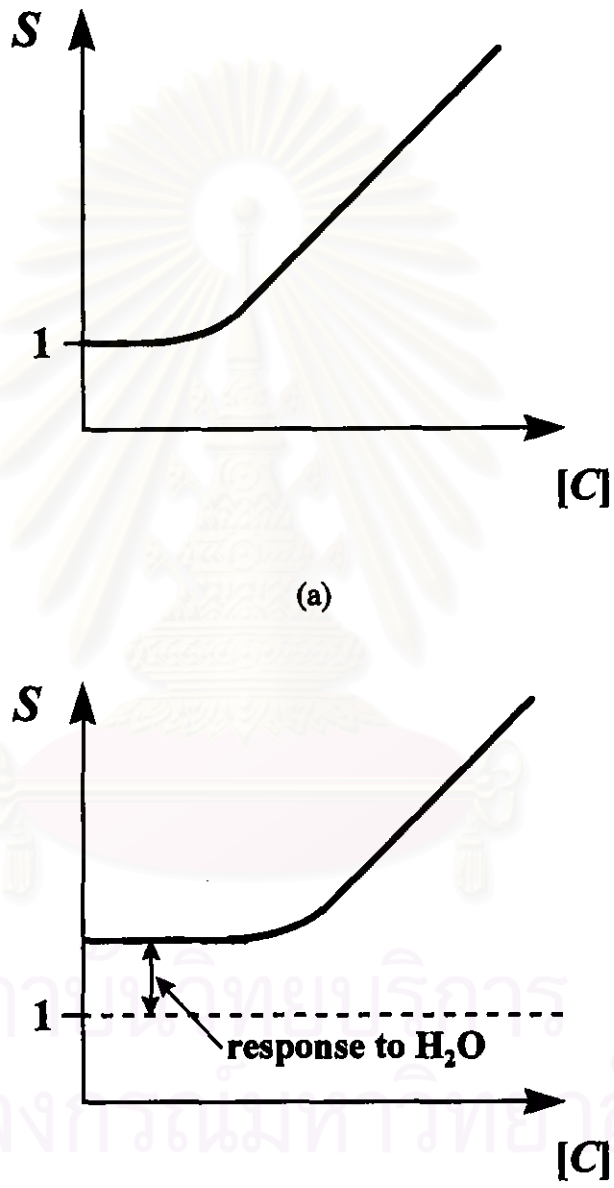

Fig. 6.1 Calibration curve for the case of (a) gas sample is calibrated with air and (b) gas sample is calibrated with pure water in the experiments.

6.2 Characterization of Gas Sensors Fabricated from the Commercial Sol Solution

6.2.1 Effect of Film Thickness

The commercial SnO_2 sol solution was purchased from Mitsubishi Material Co., Ltd. According to the specification, this solution contains 6 % of SnO_2 by weight. SnO_2 thin films were prepared by using the identical processes described in chapter V (Section 5.3). The relationship between film thickness and spin speed is shown in Fig. 6.2(a), while Fig. 6.2(b) shows the relationship between film thickness and the number of spin. The data of refractive index are also depicted in Fig. 6.2. From this data, the film thickness of SnO_2 thin film could be linearly controlled by varying the number of coatings. The thickness of each layer was about 1000 Å at spin speed 3000 rpm. Here, we come to the point that what is the optimum thickness for fabricating gas sensor. This has been investigated by varying the film thickness. SnO_2 films with thickness of 1000, 3000 and 5000 Å were coated on glass substrates and followed with Ti/Pt electrode evaporated on the top surface. The schematic diagram of the sensor structure is shown in Fig. 5.10. These thin films were subjected to test their response to alcohol and the results are shown in Fig. 6.3. The alcohol concentration was fixed at 1 % by volume and the operating temperature of gas sensor was varied from 50 to 400 °C.

It should be noted that in this experiment, the values of sensitivity were calculated from the conventional measuring circuit (see Chapter III and IV). Thus, the values of sensitivity shown in this section, are not the corrected values. However, we used only their tendency to find out the optimum thickness. In the following sections, all of experiments were performed on the new proposed measuring circuit.

The results showed that the sensitivity to alcohol of gas sensors increased slightly with the film thickness. However, there was a significant decrease in the ratio of the alcohol signal to the water signal as shown in Fig. 6.3(b). This means that the thicker films were easy to be interfered by with water or humidity. Therefore, the SnO_2 film with thickness of 1000 Å was preferable to use as a sensitive layer.

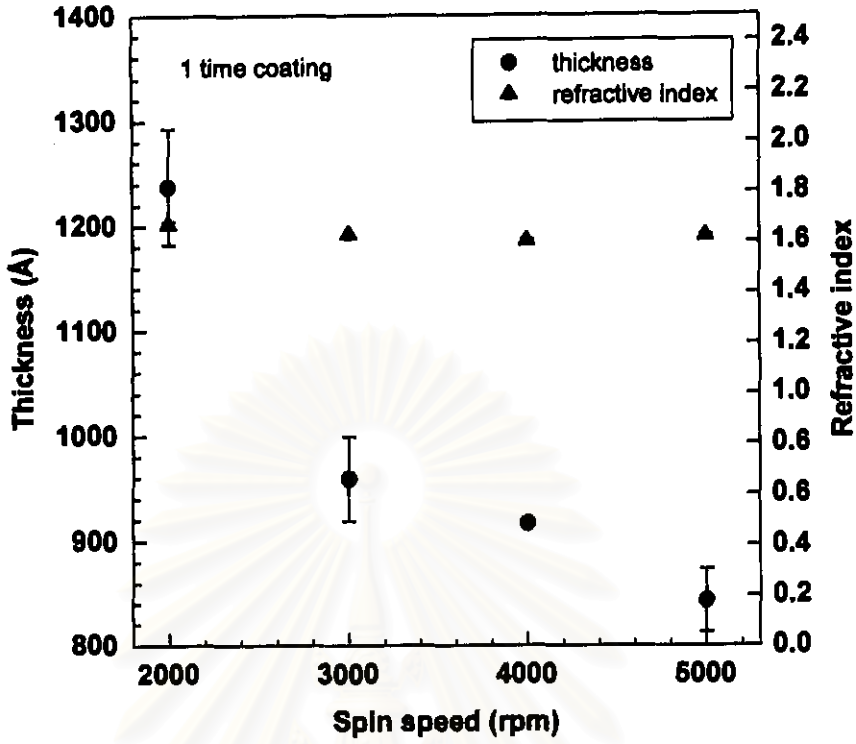

(a)

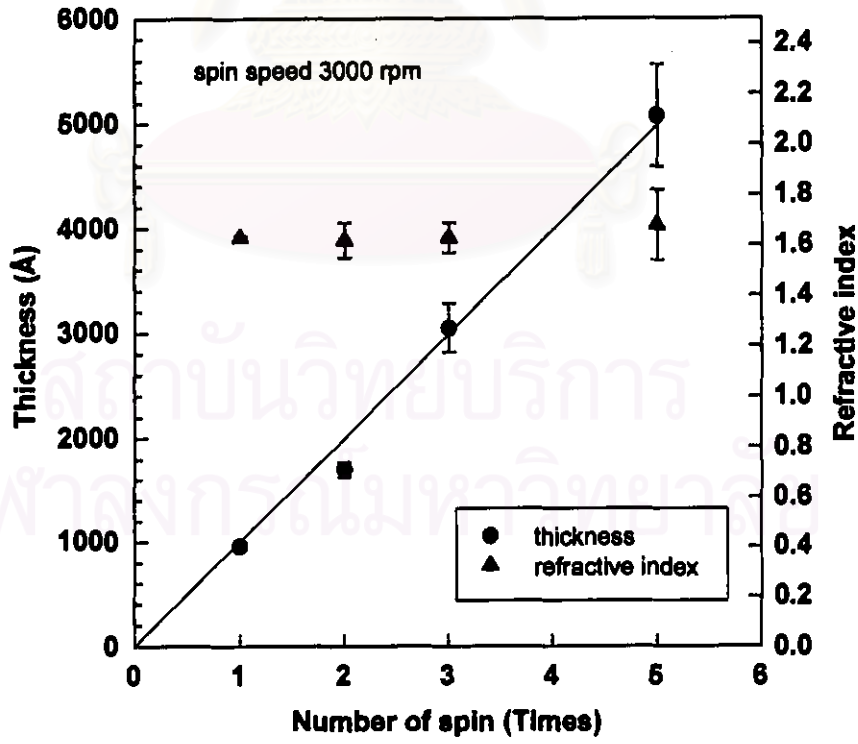

(b)

Fig. 6.2 Plot of film thickness and refractive index as a function of (a) spin speed and (b) the number of speed.

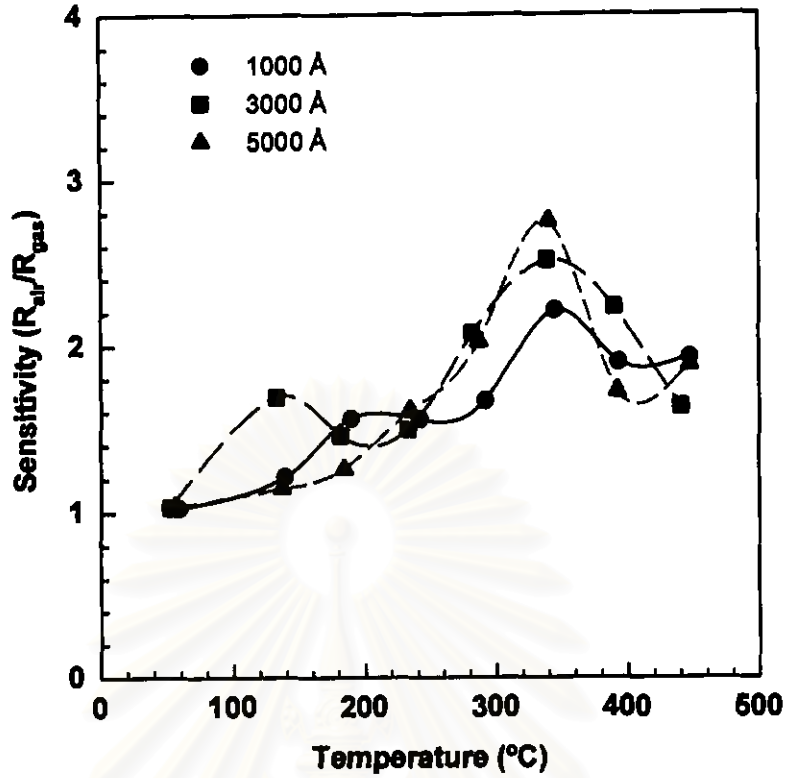

(a)

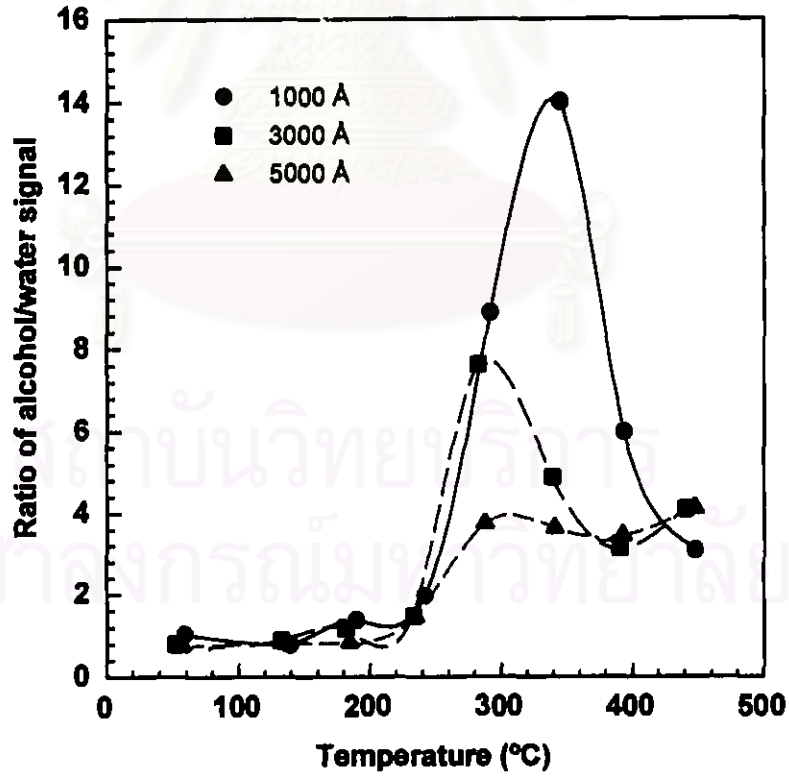

(b)

Fig. 6.3 Effect of film thickness on gas response (a) sensitivity and (b) signal of alcohol to water.

6.2.2 Response of Unmodified SnO_2 Gas Sensor

In the previous section, we had determined the optimum thickness of SnO_2 film for fabricating gas sensor. Firstly, the unmodified SnO_2 (pure SnO_2) sensors were fabricated and their gas responses to alcohol and ammonia were characteristics. The typical response curves of alcohol and ammonia are demonstrated in Fig 6.4(a) and 6.4(b) respectively. The concentration of the tested samples was varied from 0.01-10 % by volume. It was clear from Fig. 6.4 that after a tested sample was injected into the test system, there was an abrupt change in the sensor conductance due to gas adsorption. In the case of alcohol, the output voltage from the measuring circuit increased from the background voltage. This means that the resistance of SnO_2 sensor decreased. In other word, electrons were transferred from gas sample to the semiconductor surface. In contrast, this SnO_2 gas sensor showed an opposite response when it was exposed to ammonia. Although, there was a positive spike in the output voltage (a decrease in resistance) in the first part, then the output voltage continued to decrease and reach a minimum before returning to the background voltage.

Fig. 6.5 shows sensitivity of the unmodified SnO_2 sensors to alcohol and ammonia at different operating temperature. The operating temperature was varied from 150-400 °C, and the concentration of alcohol and ammonia was set to 10 % by volume. At temperature below 150 °C, the unmodified SnO_2 sensors gave no response to alcohol or ammonia solution. It was clear that the unmodified sensors gave the maximum sensitivity to alcohol and minimum sensitivity to ammonia at about 350 °C.

The calibration curves for alcohol and ammonia at 350 °C are given in Fig. 6.6. When the concentration of the test sample was increased, unmodified SnO_2 sensor showed a positive response to alcohol and a negative response to ammonia. The power law model (Eq. (6.3)) was used to fit the measured data to produce the solid lines of Fig. 6.6. Table 6.2 lists all fitted parameters. In the third column of Table 6.2, the values in parentheses show $1/k$ values.

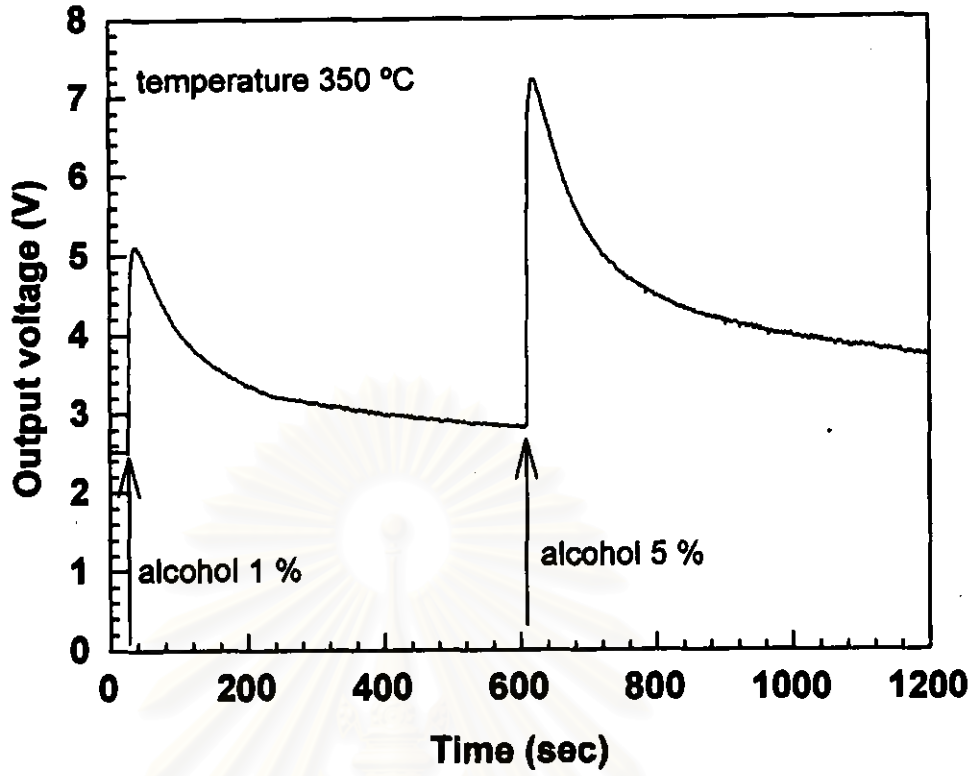

(a)

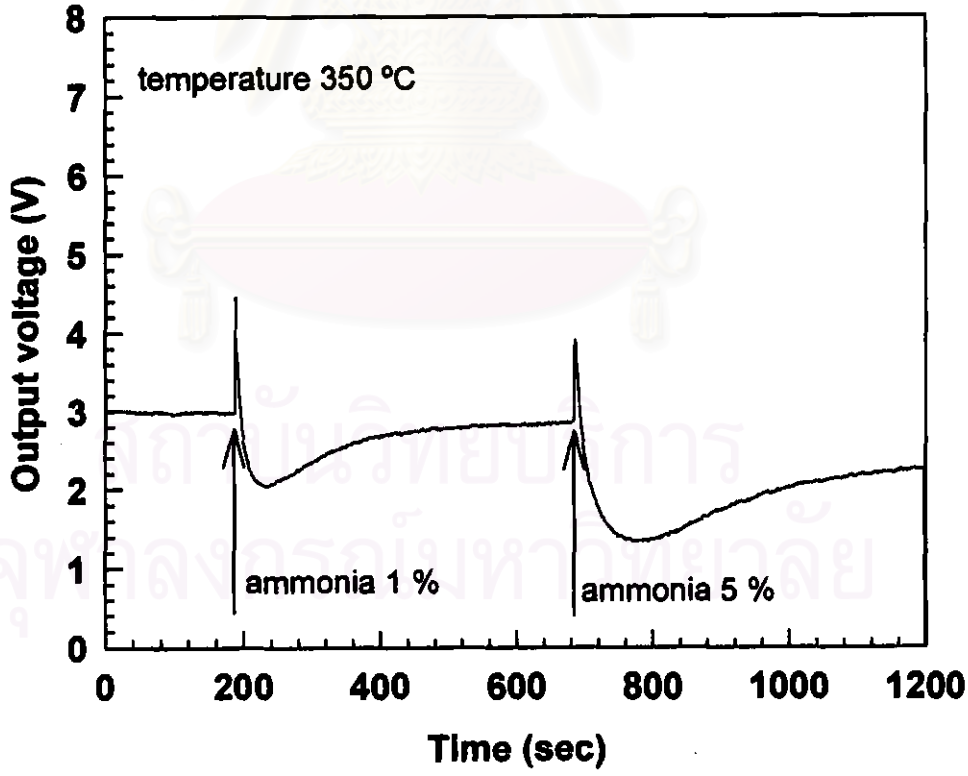

(b)

Fig. 6.4 Typical response curves of unmodified SnO_2 gas sensors (a) to alcohol and (b) to ammonia.

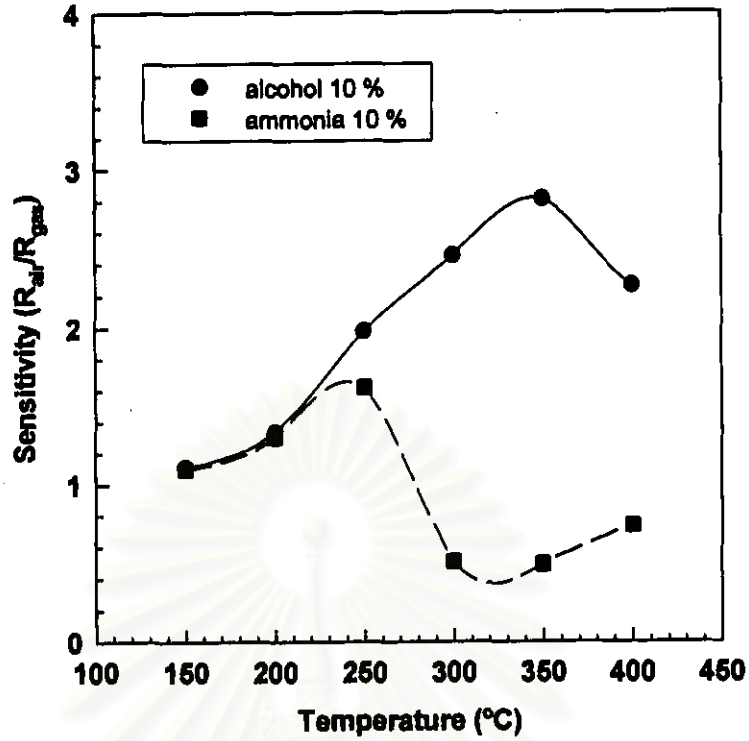

Fig. 6.5 Variation of sensitivity of unmodified SnO_2 sensor operating at different temperature.

Table 6.2 Parameters described by power law model of the unmodified SnO_2 gas sensor.

Sample	*a*	*k (1/k)*	*β*
alcohol	1.5596	11.4270 (0.09)	0.1208
ammonia	1.3596	8.2914 (0.12)	-0.2679

From Table 6.2, the threshold of the unmodified SnO_2 gas sensors for alcohol and ammonia are 0.09 and 0.12 % by volume respectively. Thus, the unmodified SnO_2 sensors could detect the concentration of alcohol and ammonia from 0.09-10 % and 0.12-10 % by volume respectively. However, in the total view, the unmodified SnO_2 sensors had low sensitivity to aicohol and ammonia.

Fig. 6.7 shows the plot of recovery time as a function of gas concentrations. SnO_2 sensor showed a nearly constant recovery time at low to moderate concentrations and an abrupt increase of recovery time at high concentrations.

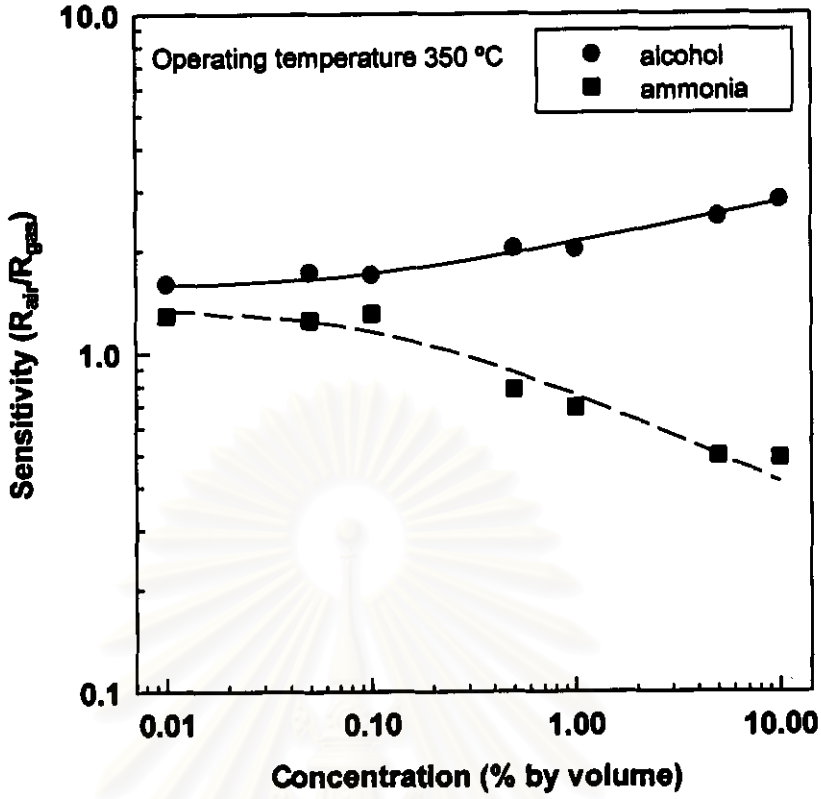

Fig. 6.6 Calibration curve of unmodified SnO_2 sensor at 350 °C.

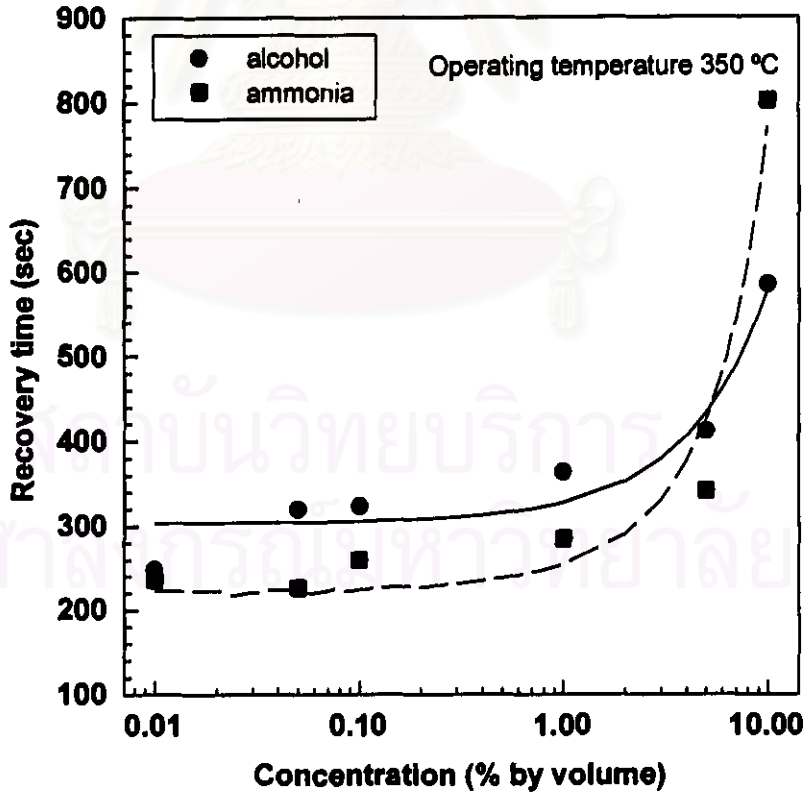

Fig. 6.7 Plot of recovery time against gas concentrations of unmodified SnO_2 sensor at 350 °C.

6.2.3 Improvement of Sensitivity by Addition of Modified Substances

In order to improve the sensitivity and selectivity of SnO_2 sensors, some modified substances had been cooperated into SnO_2 thin films. With the advantage of sol-gel technique, we could expect that the modified substances will be well dispersed into SnO_2 thin film. Table 6.3 lists the modified substances used in the experiments.

Table 6.3 Lists of modified substance used in the experiments.

Substances	% by weight	Solvent
$AgNO_3$	5	methanol
$FeCl_3$	5	methanol
Au	0.1-1%	$HCl:NO_3$ dilute with methanol

Firstly, the optimum concentration of Au in SnO_2 film was investigated. Fig. 6.8 shows the change of sensitivity and recovery time as a function of Au concentration. The SnO_2 sensors modified with 0.1 % Au (Au-SnO_2) gave the highest sensitivity. From Fig. 6.8(b), the recovery time had a tendency to increase with the amount of Au in SnO_2 films.

Fig. 6.9 compares the sensitivity of various modified SnO_2 films in terms of the operating temperature. It should be remarked that the best results are obtained from Au modified SnO_2 film (Au-SnO_2). As can be seen from Fig. 6.9 that the addition of $AgNO_3$ hardly affected the response characteristics of SnO_2 to alcohol and ammonia. The addition of $FeCl_3$ and Au increased the sensitivity of SnO_2 films to alcohol about 2 times comparing with the unmodified SnO_2 sensor. It can be observed from Fig. 6.9 that all of various SnO_2 sensors showed the optimum operating temperature at 350 °C. Fig. 6.10 compares calibration curves of the various modified

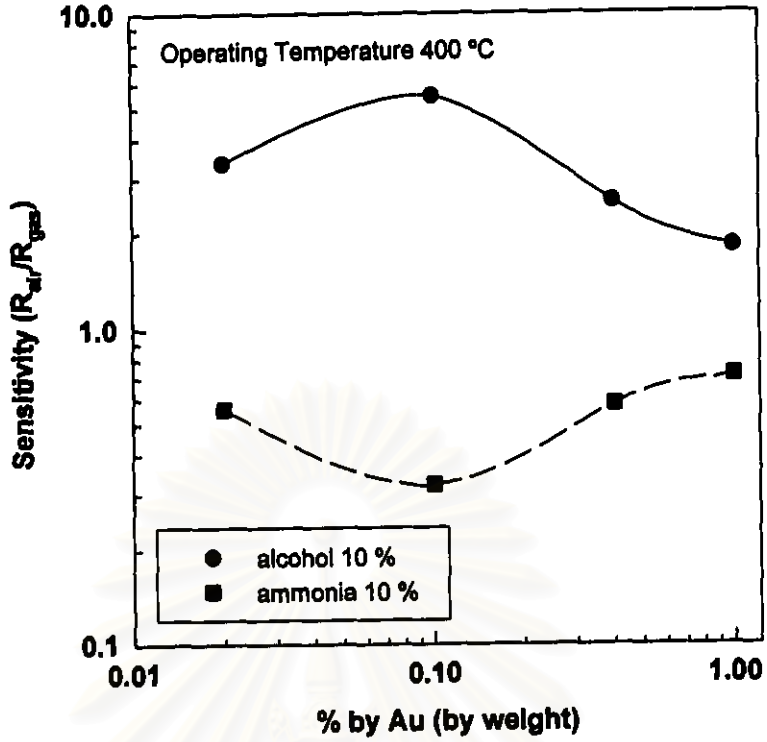

(a)

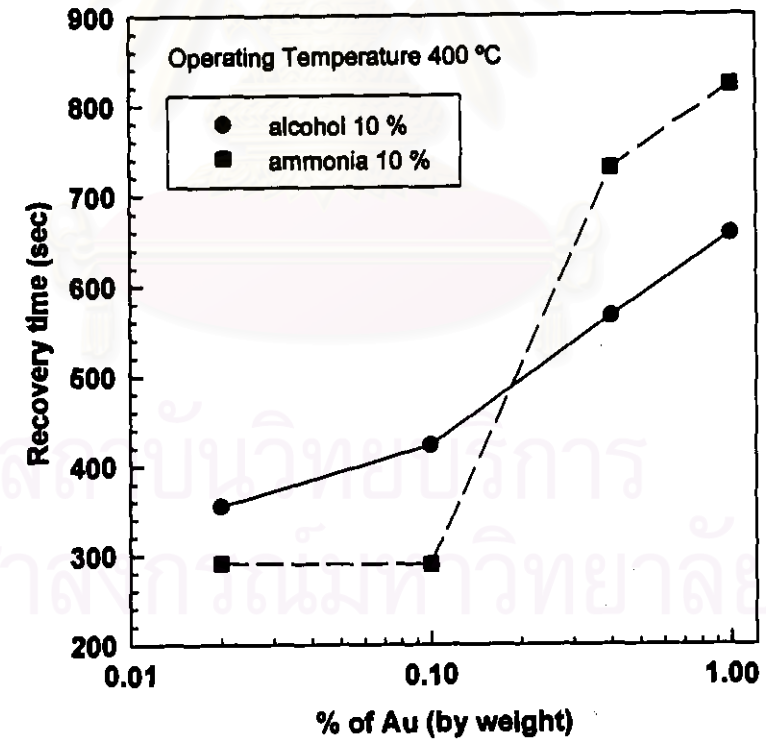

(b)

Fig. 6.8 Variation of (a) sensitivity and (b) recovery as a function of Au concentration.

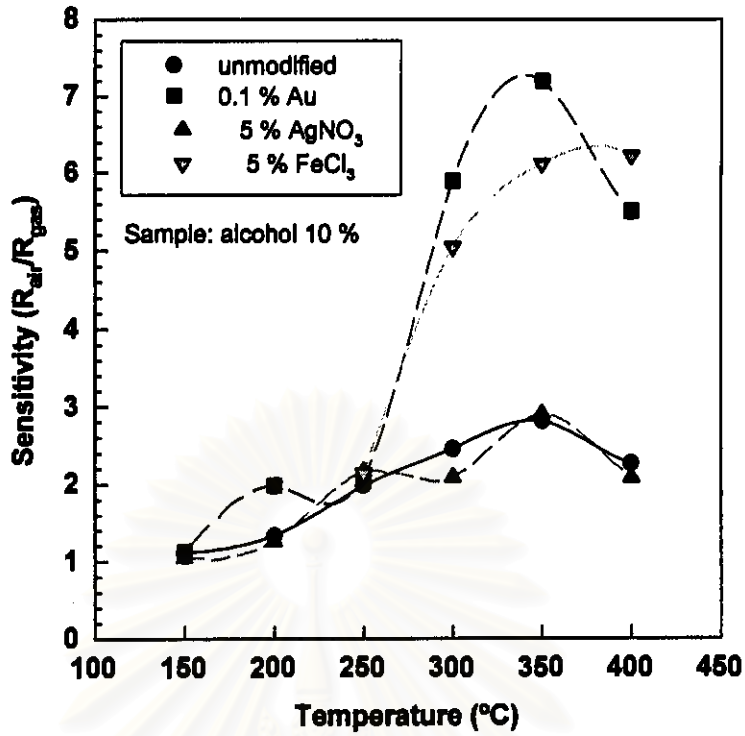

(a)

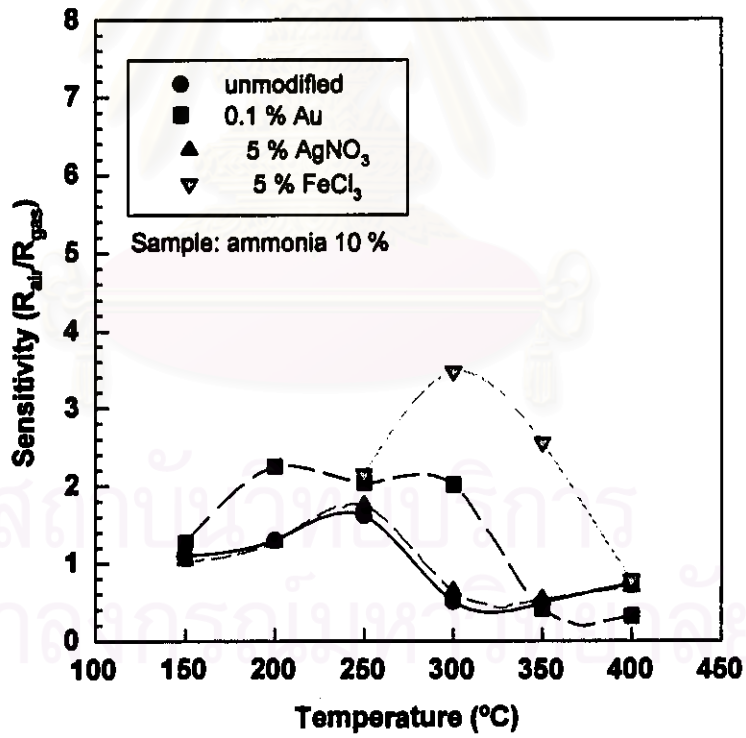

(b)

Fig. 6.9 Sensitivity of various modified SnO_2 sensors to (a) alcohol and (b) ammonia at different operating temperature.

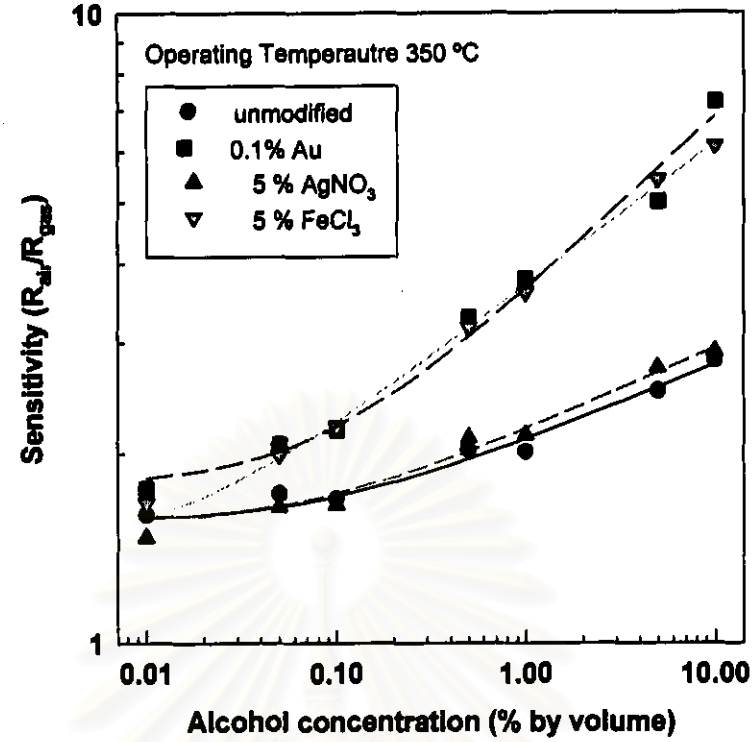

(a)

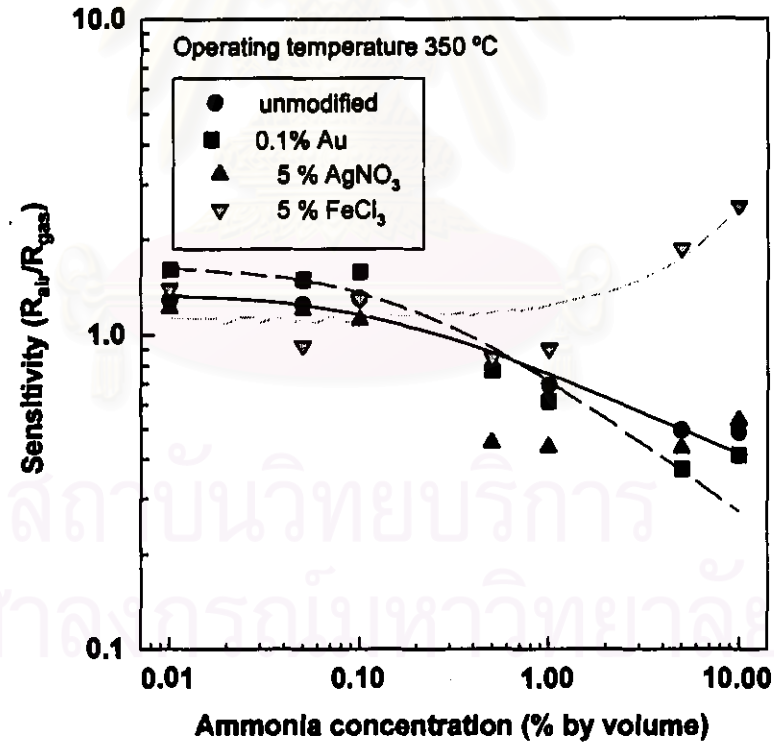

(b)

Fig. 6.10 Calibration curve of various modified SnO_2 sensors for (a) alcohol and (b) ammonia.

SnO_2 sensors to alcohol and ammonia. Table 6.4 lists the parameters expressed in Eq. (6.3) for various SnO_2 gas sensors. These parameters were used to fit with the data as represented by the various lines in Fig. 6.10. It is noted that in the case of the $AgNO_3$-SnO_2 gas sensor for the detection of ammonia, the experimental results could not be predicted by the power law model.

Table 6.4 Parameters of power law model for various SnO_2 gas sensors.

Sample	Sensor	a	k	β
alcohol	unmodified	1.5596	11.4270 (0.09)	0.1208
	0.1 % Au	1.7698	12.0734 (0.08)	0.2812
	5 % $AgNO_3$	1.5518	12.9156 (0.08)	0.1312
	5 % $FeCl_3$	1.3893	74.3815 (0.01)	0.2258
ammonia	unmodified	1.3596	8.2914 (0.12)	-0.2679
	0.1 % Au	1.6636	5.9192 (0.17)	-0.4414
	5 % $AgNO_3$	-	-	-
	5 % $FeCl_3$	1.1292	0.8410 (1.19)	0.5762

From Table 6.4, the values of a from various gas sensors were not so different, this means that the responses to pure water were at the same level for all sensors. From the k and β values, $FeCl_3$-SnO_2 sensor gave the best results for detection of alcohol, while Au-SnO_2 sensor was suitable for ammonia detection. $FeCl_3$-SnO_2 could detect alcohol concentration ranging from 0.01-10 % by volume, while Au-SnO_2 could detect ammonia concentration ranging from 0.2 - 10 % by volume.

The plots of recovery time against concentration are given in Fig. 6.11. It is clear that the recovery time of all sensors was nearly constant at low to medium concentration and increased rapidly at high concentration.

The experiments done on the commercial sol has revealed the feasibility to use the sol-gel technique as one of the key technology in gas sensors fabrication. In the

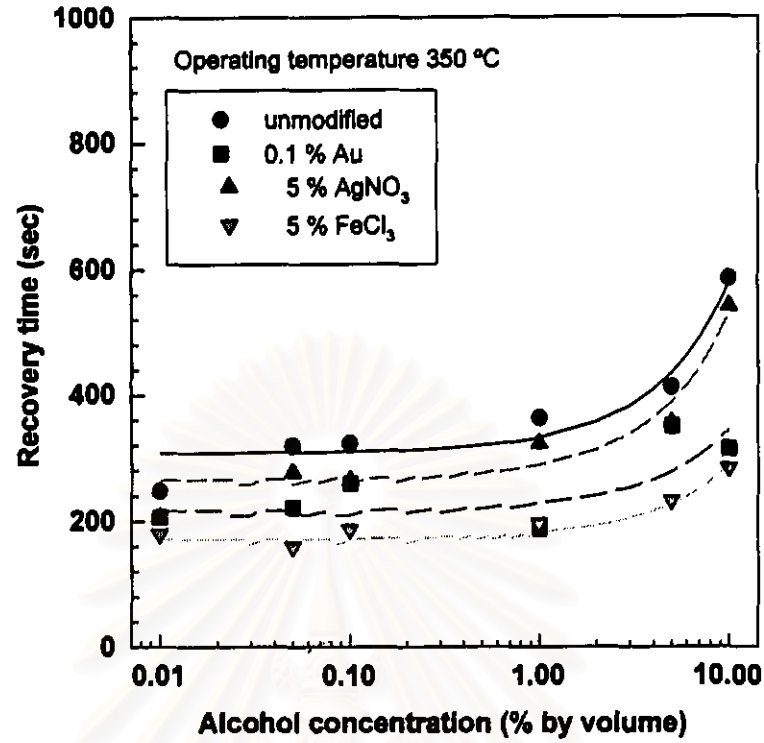

(a)

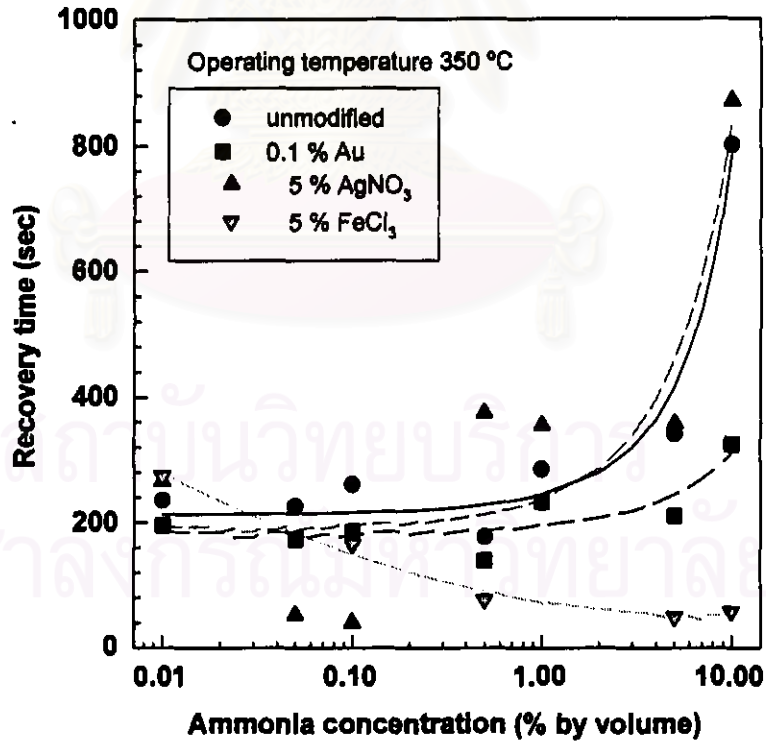

(b)

Fig. 6.11 Recovery time of various modified SnO_2 sensors for (a) alcohol and (b) ammonia.

overall views, SnO_2 gas sensors fabricated of this sol showed low sensitivity, however, a good detection limit. In the next section, the experimental results of SnO_2 sensors prepared from the simply developed sol will be presented.

6.3 Characterization of Gas Sensors Prepared from the Simple Mixed Sol

The unmodified and $CuSO_4$ modified SnO_2 ($CuSO_4$-SnO_2) films were prepared from the sol solution synthesized by the simple mixed processes. The amount of $CuSO_4$ was varied from 0.001 - 1 % by weight. The data of film thickness and refractive index as a function of percentage of $CuSO_4$ are shown in Table 6.5. Because the uniformity of these films (see Fig. 5.3) was not so good, the fluctuation of thickness and refractive index could be observed.

Table 6.5 Film thickness and refractive index at different amount of $CuSO_4$.

% of $CuSO_4$	Thickness (Å)	Refractive index
0	1133	1.360
0.001	791	1.648
0.01	715	1.663
0.1	709	1.557
1	703	1.444

Fig. 6.12 shows the typical response characteristics of the unmodified SnO_2 film. It should be noted that the response characteristics of these synthesized SnO_2 thin films showed an increase in conductivity after exposure to either alcohol or ammonia. This characteristic was contrast to that of SnO_2 prepared from the commercial sol solution. The effect of $CuSO_4$ on gas sensitivity is shown in Fig.

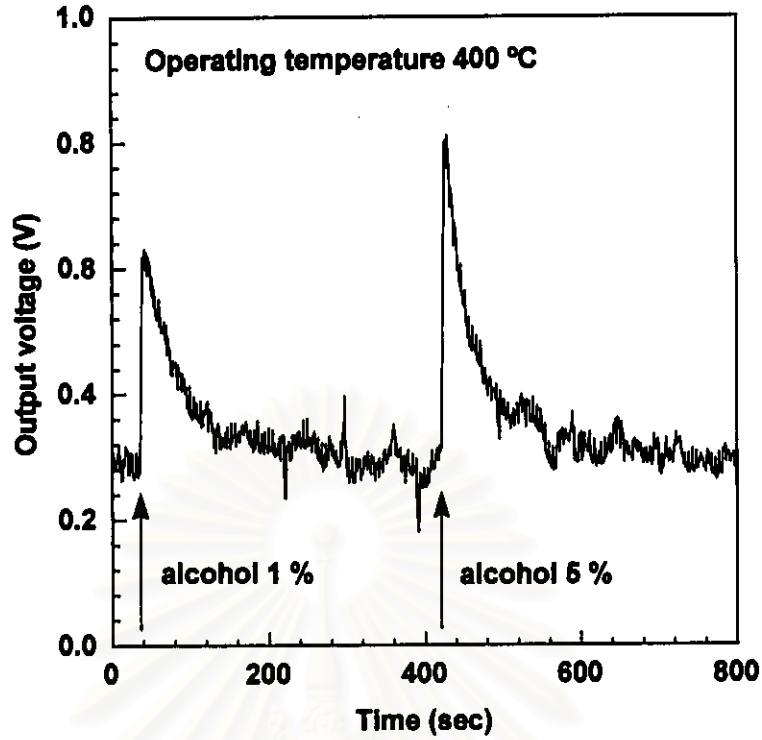

(a)

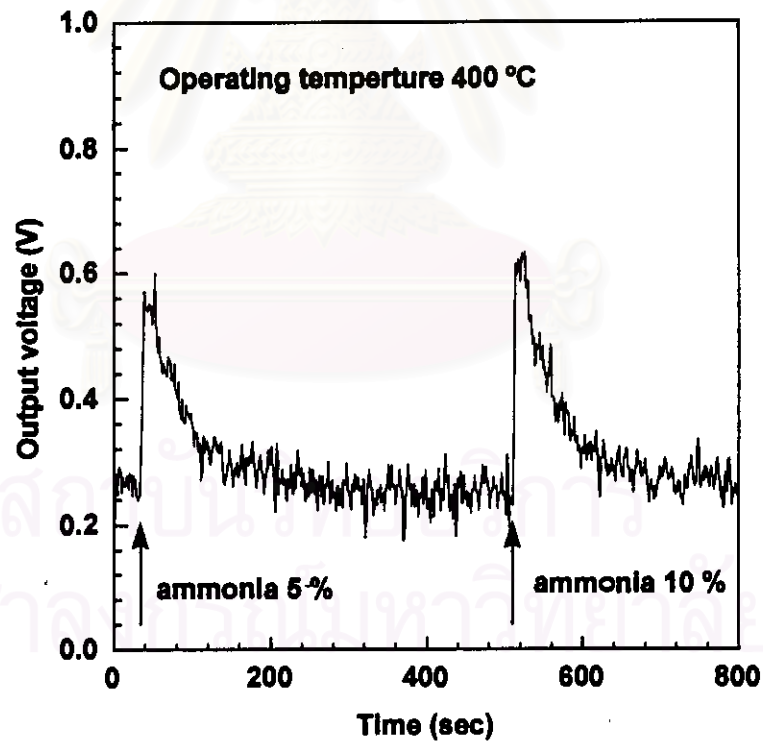

(b)

Fig. 6.12 Response characteristics of SnO_2 prepared from the simple mixed process (a) alcohol and (b) ammonia.

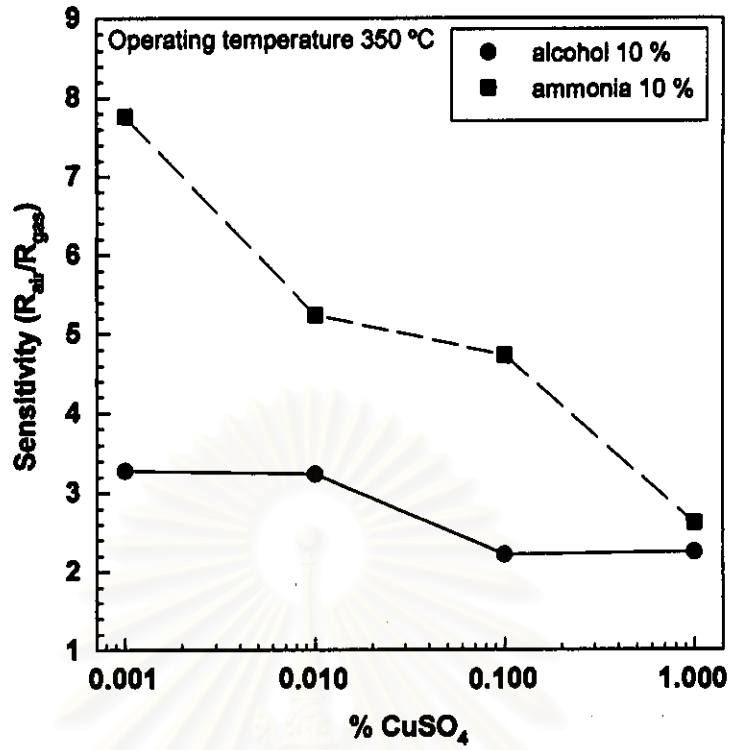

(a)

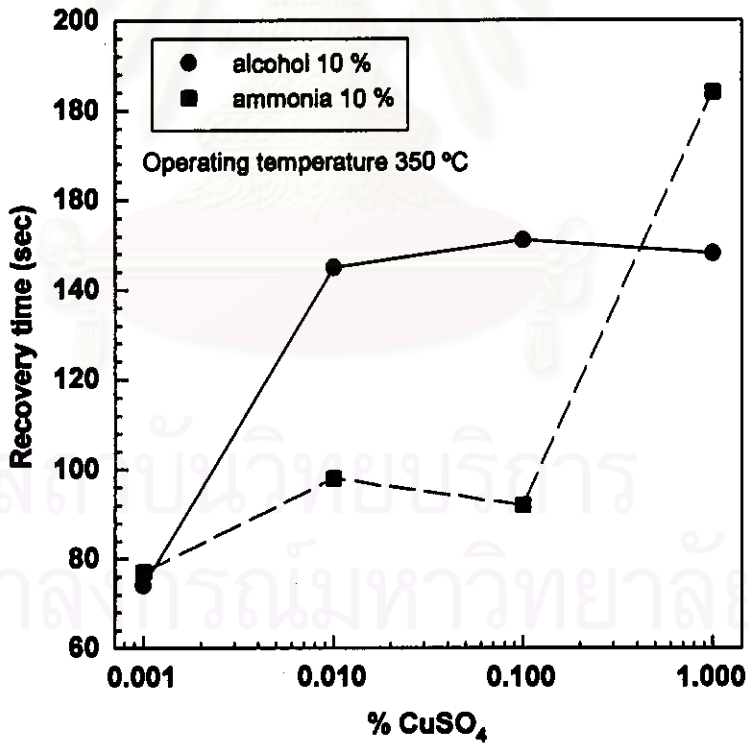

(b)

Fig. 6.13 Variation of (a) sensitivity and (b) recovery time as a function of the percentage of $CuSO_4$ in SnO_2 films.

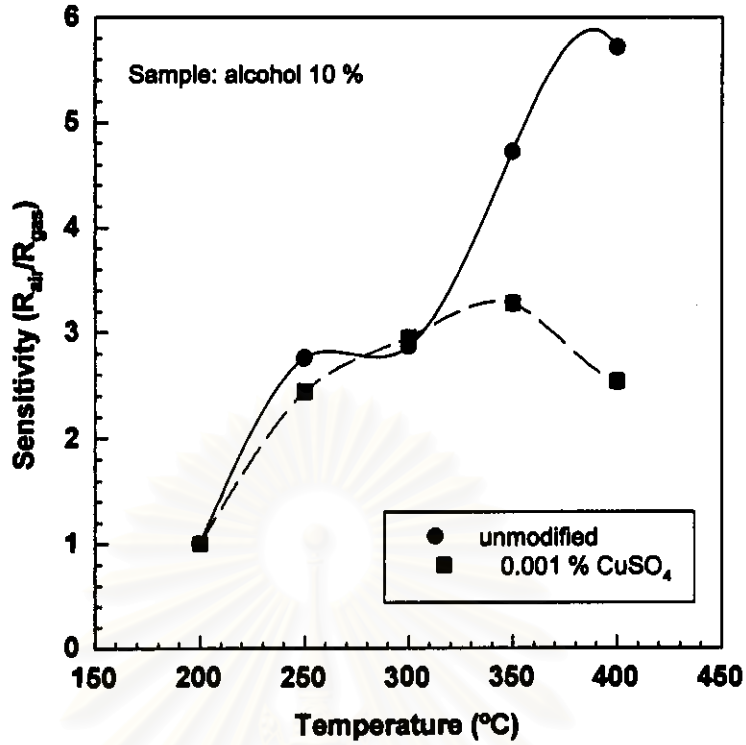

(a)

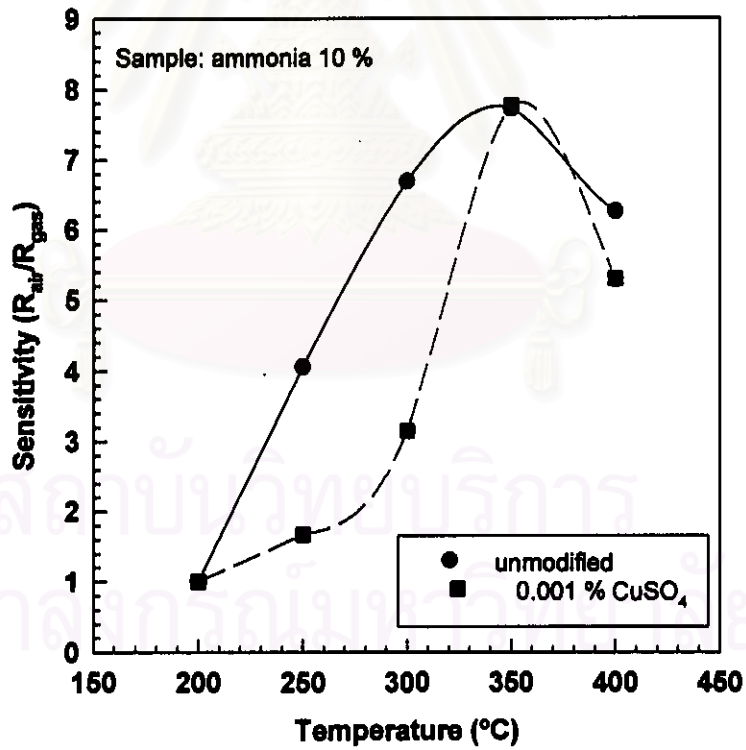

(b)

Fig. 6.14 Variation of sensitivity and recovery time as a function of temperature for SnO_2 sensors.

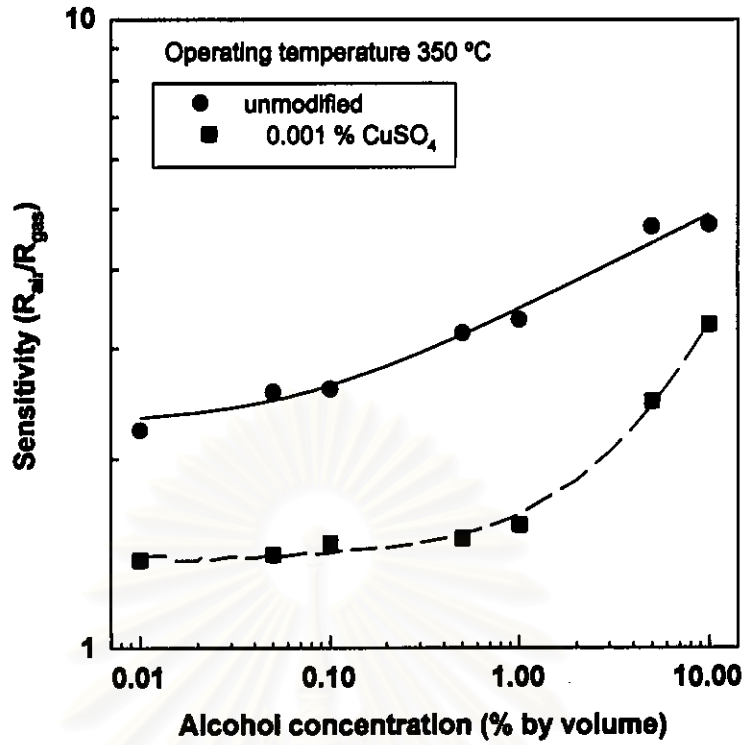

(a)

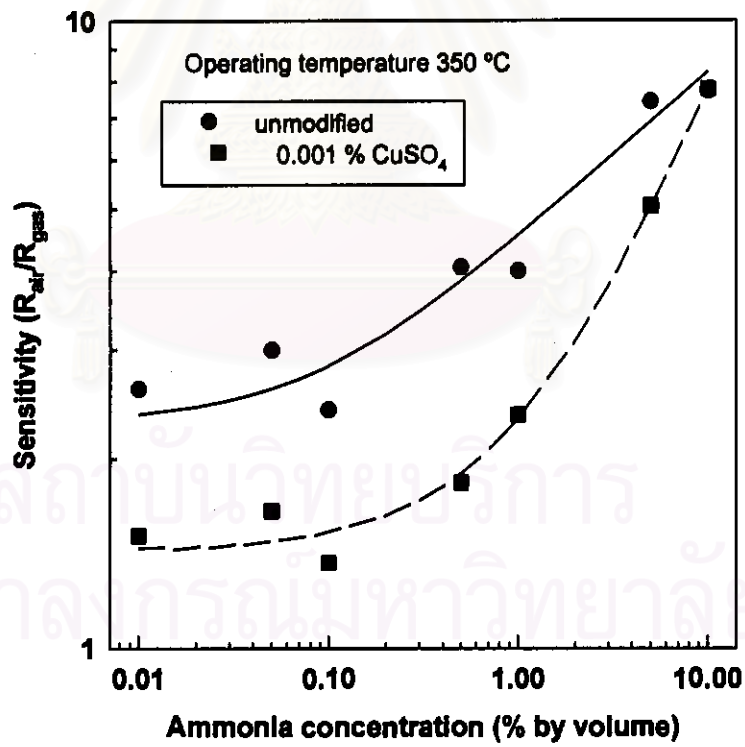

(b)

Fig. 6.15 Calibration curves for SnO_2 sensors to (a) alcohol and (b) ammonia.

6.13. The results in Fig. 6.13 showed that the cooperation of $CuSO_4$ into SnO_2 films reduced the sensitivity to both alcohol and ammonia, while recovery time seemed to increased with the percentage of $CuSO_4$. Thus, the SnO_2 with 0.001 % $CuSO_4$ gave the highest sensitivity to both alcohol and ammonia. Fig. 6.14 shows comparison of sensitivity of the unmodified SnO_2 and 0.001 % $CuSO_4$-SnO_2 sensors at the different operating temperature. It could be observed that the optimum temperature of both sensor was the same at 350 °C. The calibration curves for these two sensors at 350 °C are shown in Fig. 6.15. Table 6.6 lists all parameters involving in power law model for the unmodified SnO_2 and 0.001 % $CuSO_4$-SnO_2 sensors. According to Table 6.6, the values of *a* parameter of the unmodified films was about two times greater than to that of the 0.001 % $CuSO_4$-SnO_2 film, this means that the former film was easy to response to water or humidity than the later. However, looking at the *k* values, we can conclude that the unmodified films could detect alcohol ranging from 0.07-10 % and ammonia from 0.08 - 10 %, while the $CuSO_4$-SnO_2 film could detect alcohol from 3.89 - 10 % and 1-10 %. The changes of recovery time with alcohol and ammonia concentration are not shown here, because the data are too scattered and can not be interpreted. It should be remarked that the signals obtained these sensors (Fig. 6.12) showed some fluctuations. This caused some error in the calculation of recovery time. In conclusion, the SnO_2 thin film gas sensors fabricated by the simply mixed sol showed a low sensitivity and high detection limit. However, the unacceptable disadvantage of these senseors was the unstability of sensor signals. The sensor signal showed high fluctuation as can be seen in Fig. 6.12.

Table 6.6 Parameters of power law model for unmodified SnO_2 and 0.001 % $CuSO_4$-SnO_2 gas sensors prepared from simple mixed process.

Sample	Sensor	*a*	*k (1/k)*	*β*
alcohol	unmodified	2.2846	14.4553 (0.07)	0.1526
	0.001 % $CuSO_4$	1.3989	0.2565 (3.89)	0.6717
ammonia	unmodified	2.2917	11.8695 (0.08)	0.2635
	0.001 % $CuSO_4$	1.4357	0.9536 (1.05)	0.7170

6.4 Characterization of Gas Sensors Prepared from the Rigorously Controlled Sol

In this section, we will discuss about the characterizations of gas sensors obtained from the rigorously controlled sol. The rigorouslly controlled sol has been developed, since the sensors prepared from the simple mixed sol showed the unstability in sensor signals.

6.4.1 Effect of Film Thickness

The effect of film thickness on gas response of the unmodified SnO_2 sensors was investigated to find the optimum thickness for fabricated gas sensors. The film thickness could be controlled linearly by varing the number of coatings (Fig. 5.9). The thickness of each coating was about 350 Å. The effect of film thickness on gas response to alcohol and ammonia are shown in Fig. 6.16. The number of coatings was varied from 1, 2, 3 and 4 times which are equivalent to the film thickness of 366, 714, 1056 and 1325 Å respectively. It is clear that the sensitivity increased with the film thickness. We interpreted these results as the surface area of SnO_2 increased with the film thickness. Fig. 6.17 summarizes the effect of the film thickness on sensitivity and recovery time at 350 °C. It should be noticed that recovery time decreased as the film thickness increased. At this state, it is still difficult to explain this phenomena. From these results, we determined to use SnO_2 films with thickness about 1000 Å (the number of coatings = 3), since it provides a rather high sensitivity and fast recovery time. Although, the thicker film resulted in the higher sensitivity but it would take a more complicated and longer processes for more thicker film thickness.

6.4.2 Current-Voltage Characteristic

The *I-V* characteristics of the unmodified SnO_2 films with various film thickness were investigated at different operating temperature. An example of *I-V*

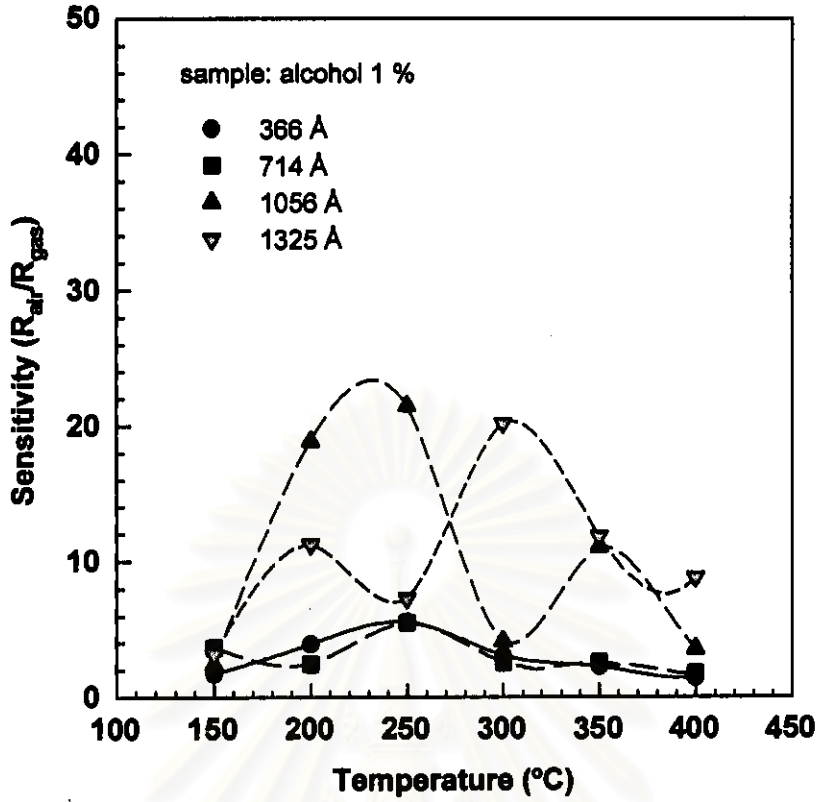

(a)

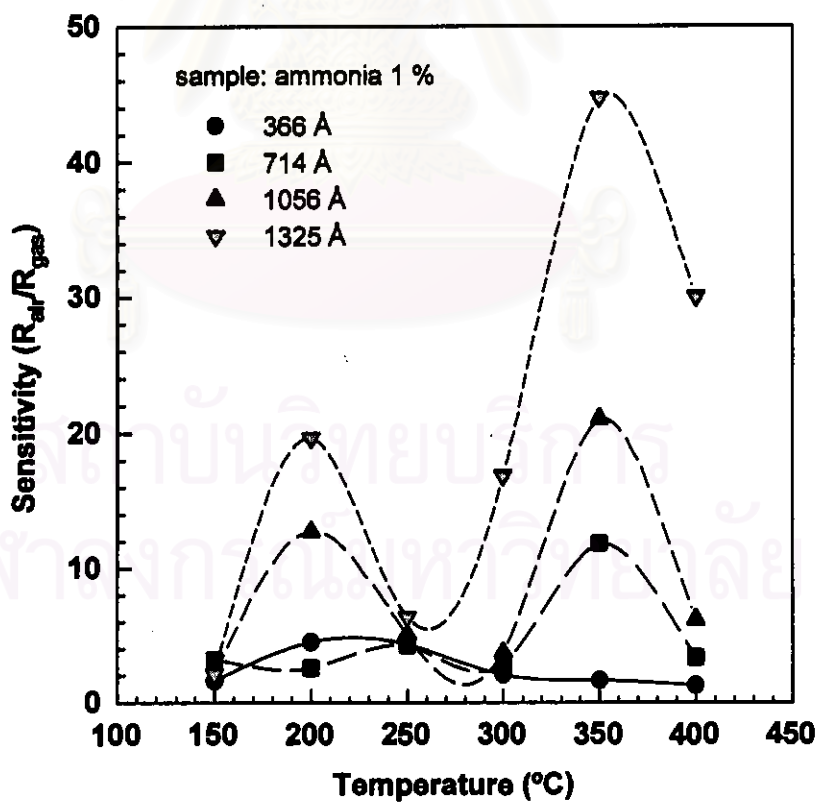

(b)

Fig. 6.16 Plot of sensitivities versus temperature as a function of film thickness for (a) alcohol and (b) ammonia.

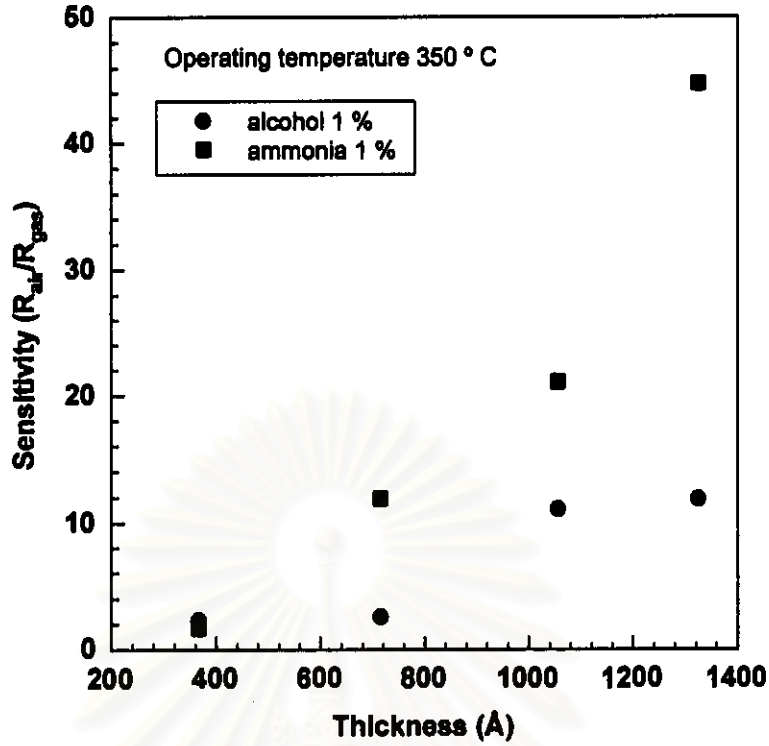

(a)

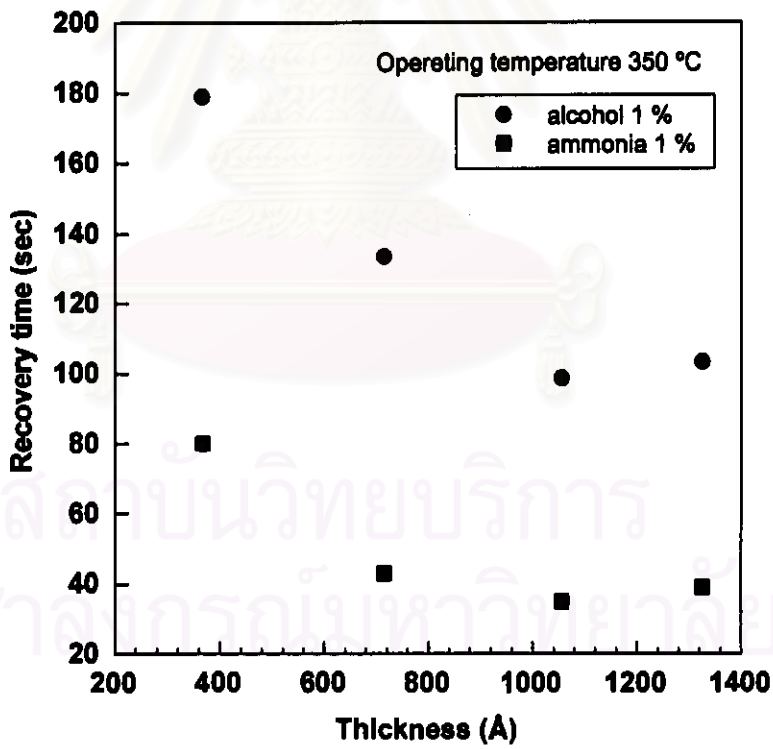

(b)

Fig. 6.17 Plot of (a) sensitivity versus film thickness and (b) recovery time versus film thickness.

characteristic in synthetic air is shown in Fig. 6.18. The *I-V* characteristic of the fabricated gas sensors showed the non-linear relation described by the empirical equation given in Eq.(4.6). Fig. 6.19 shows the Arrhenius plots of the sensor conductivity as a function of film thickness. Since, the gas sensors possess the non-linear characteristic, therefore conductivity varies with the voltage across sensor, V_s. The values of sensor conductivity shown in Fig. 6.19 were calculated at V_s = 5 V, since, all gas sensors were set to operate at this voltage level in the gas response tests.

All of the curves in Fig. 6.19 exhibited the Arrhenius relation with an activation energy of 0.85 eV. According to Morrison model[9], the conductance, G of ceramic material at a temperature, T may be described by

$$G = G_o \exp(-qV_s / kT) \tag{6.2}$$

where qV_s is the surface potential barrier energy at grain boundary and G_o is a factor that includes the intergranular conductance and may be considered as temperature insensitive term when compared to the exponential factor. Therefore, the value of activation energy is corresponding to the value of surface potential. The band diagram at grain boundary deduced from these results is shown schematically in Fig. 6.20. It is important to note that the band gap of SnO_2 is 3.7 eV[82].

It should be noted that the sensor conductance decrease as the film thickness increased. This supports the assumption that the porosity of the thin film increased with the film thickness, especially at the interface of interconnected layer. In other word, the adhesion of each layer was not so good that the conductance decreased as the film increased. Uozumi et al. reported the enhancement of gas sensitivity by increase the material porosity[83]. Thus, the increase of gas sensitivity with the film thickness, perhap, due to from the porosity.

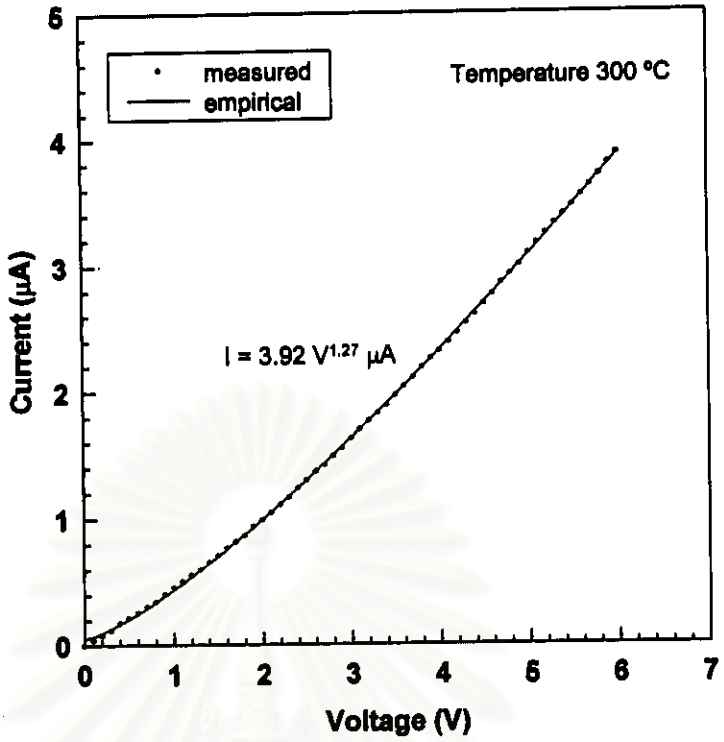

Fig. 6.18 Example of *I-V* characteristic of the fabricated gas sensor in synthetic air.

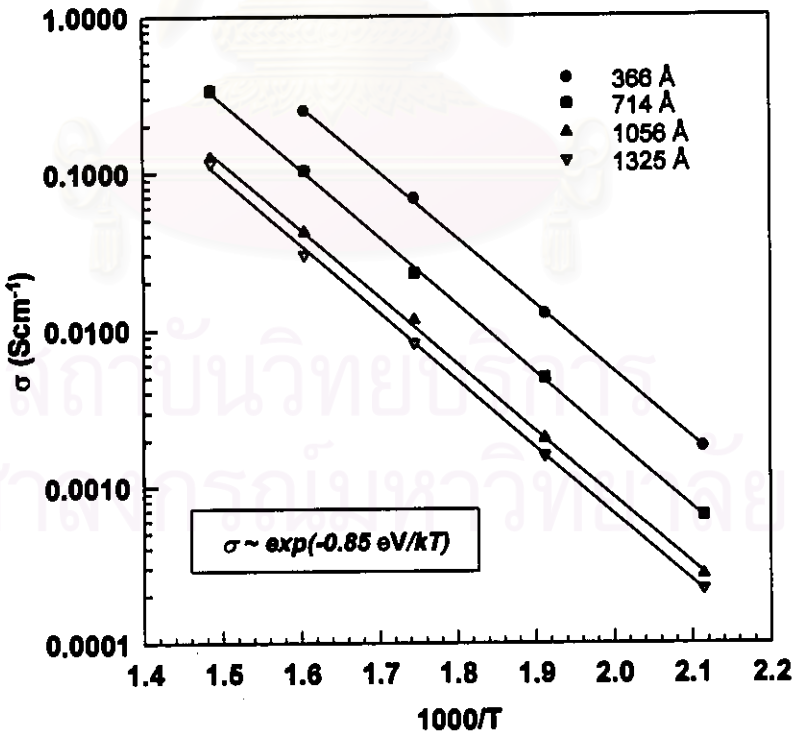

Fig. 6.19 Arrhenius plot of sensor conductance for SnO_2 films with different film thickness.

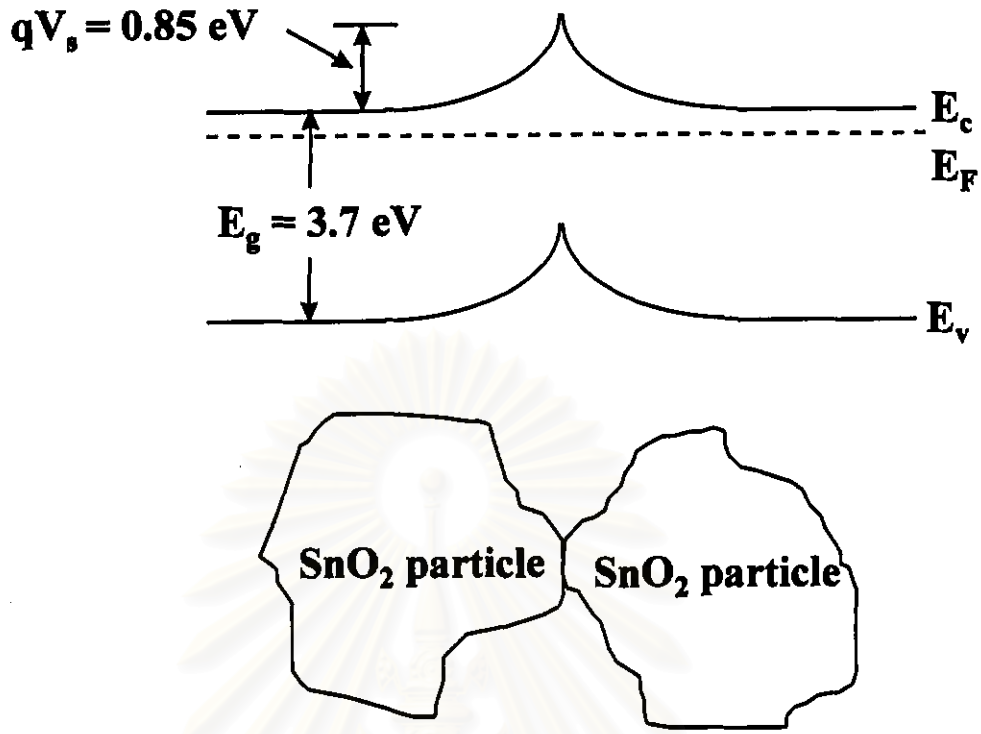

Fig. 6.20 Schematic picture of the contact between two SnO_2 particles and the formation of an energy barrier.

6.4.3 Response of Gas Sensors

Five kinds of SnO_2 gas sensors had been fabricated from this sol solution prepared by the rigorously controlled process. These were the unmodified SnO_2, $CuSO_4$-SnO_2, Au-SnO_2, $AgNO_3$-SnO_2 and $FeCl_3$-SnO_2 gas sensors. The amount of modified substance, i.e. $CuSO_4$, Au, $AgNO_3$ and $FeCl_3$ in SnO_2 films was varied from 0.001-1 % by weight. These modified substance were firstly dissolved in alcoholic solvent and then mixed homogeneously into the mother sol solution of tin alkoxide. The amount of modified substance in SnO_2 films were calculated from the amount of tin alkoxide dissolved in alcohol (see Chapter V). Fig. 6.21 shows the typical response characteristic of these gas sensors to alcohol and ammonia. It is remarked that all gas sensors prepared from this sol showed an increase of sensor conductance

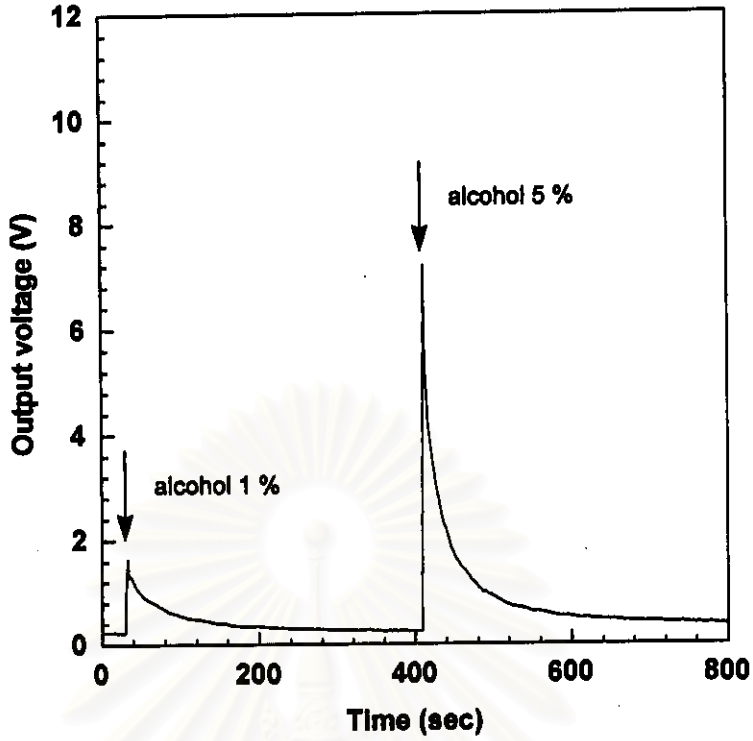

(a)

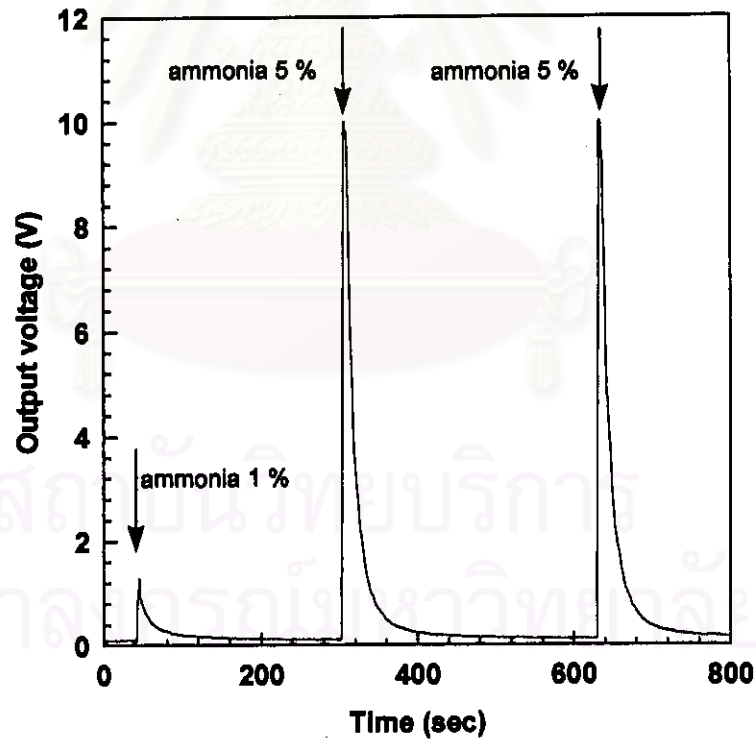

(b)

Fig. 6.21 Response characteristics of SnO_2 gas sensors prepared from the rigorously controlled process: (a) alcohol and (b) ammonia at 350 °C.

as a function of the amount of modified substances are shown in Table 6.7. The film thickness was in the range of 1000 Å by using 3 coatings.

after their exposure to either alcohol or ammonia. The data of film thickness and refractive index

Table 6.7 Film Thickness and refractive index of various SnO_2 films.

Modified substance	% by weight	Thickness (Å)	Refractive index
$CuSO_4$	0.001	1089	1.781
	0.01	840	1.788
	0.1	1026	1.774
	1	1036	1.784
Au	0.001	971.2	1.767
	0.01	1095	1.753
	0.1	1104	1.753
	1	1113	1.762
$AgNO_3$	0.001	927	1.779
	0.01	1112	1.785
	0.1	982	1.766
	1	916	1.774
$FeCl_3$	0.001	1063	1.804
	0.01	1069	1.796
	0.1	1060	1.764
	1	1119	1.775

However, these sensors will be divided into two groups and discussed separately. The first group of sensors consists of the unmodified SnO_2, $CuSO_4$-SnO_2

and Au-SnO_2 thin film gas sensors, and the second group are the unmodified SnO_2, $AgNO_3$-SnO_2 and $FeCl_3$-SnO_2 gas sensors. This division is according to the aging time of the sol solution. The sensors in the first group were fabricated from the freshly prepared sol solution. The sensors in the latter group were prepared from the sol solution which was stored for 6 months. We could not compare the performance of these two groups of sensors together, since it was found that the aging time of the sol solution had some effects on the gas sensing properties of SnO_2 sensors. However, we could still determine the effect of modified substances into SnO_2 thin film by comparing their sensing performances with the unmodified SnO_2 sensors which use as the controlling samples in each group. Thus, we will discuss our sensors into two groups according to the above statements.

6.4.3.1 $CuSO_4$-SnO_2 and Au-SnO_2 Sensors

The effects of the amount of $CuSO_4$ and Au in SnO_2 films on gas sensitivity had been investigated and their concentration were varied from 0.001 - 1 % by weight. Their responses to alcohol and ammonia as a function of $CuSO_4$ and Au were investigated and the results are shown in Fig. 6.22. It was observed that the amount of $CuSO_4$ and Au in SnO_2 films that gave the highest sensitivity was 0.001 and 0.01 % respectively.

Fig. 6.23 compared sensitivity of the unmodified SnO_2, $CuSO_4$-SnO_2 and Au-SnO_2 gas sensors as a function of operating temperature. It was clear that the addition of modified substance reduced the sensitivity to both alcohol and ammonia. The fabricated gas sensors gave the highest sensitivity at 250 °C for alcohol detection and 350 °C for ammonia. At 350 °C, the sensitivity to alcohol was almost suppressed comparing to the sensitivity to ammonia. This means that the selectivity of ammonia was enhanced in the case of $CuSO_4$-SnO_2 and Au-SnO_2. The plots of recovery time versus operating temperature are given in Fig. 6.24. The recovery time of all sensors decreased significantly as temperature increased, and the recovery time below 200 °C was unacceptably long.

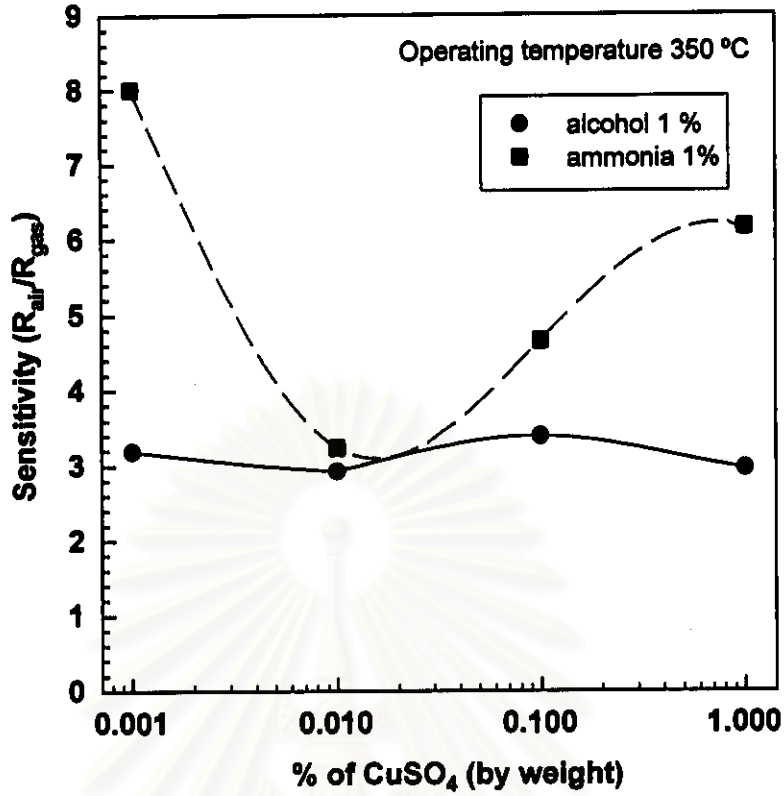

(a)

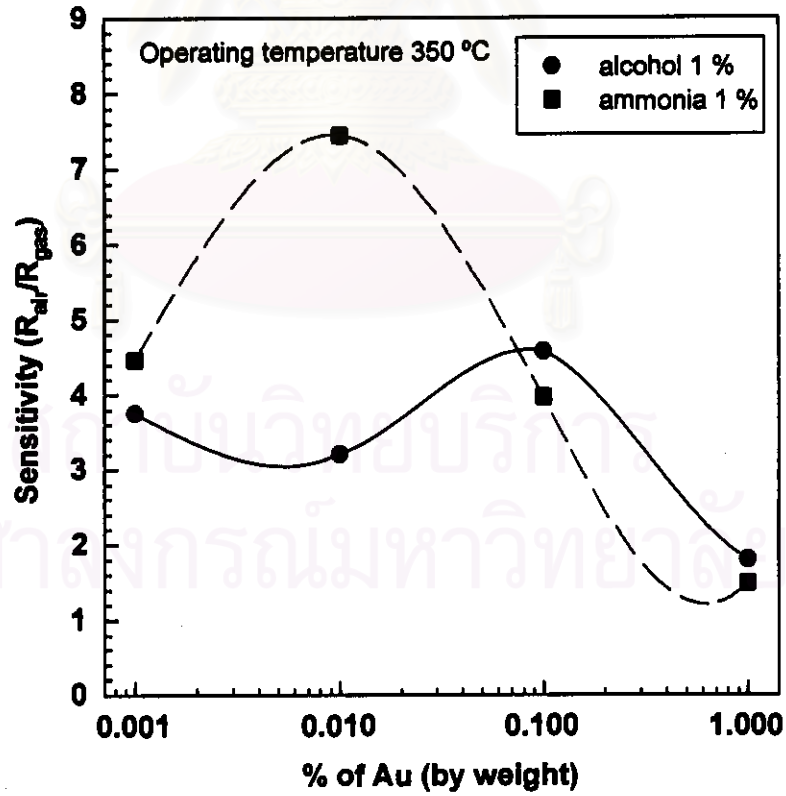

(b)

Fig. 6.22 Variation of gas sensitivity as a function of (a) $CuSO_4$ and (b) Au.

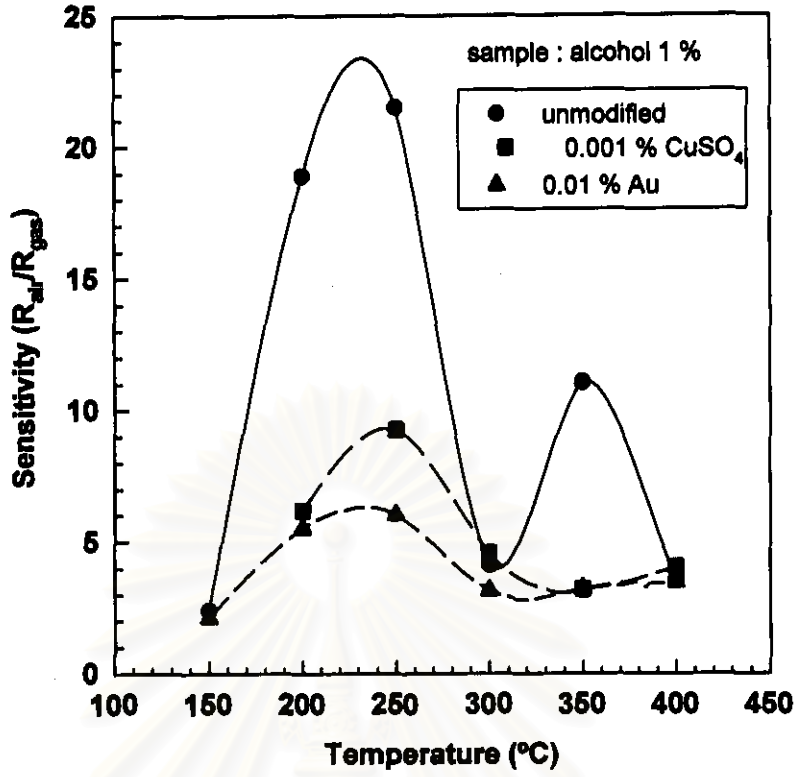

(a)

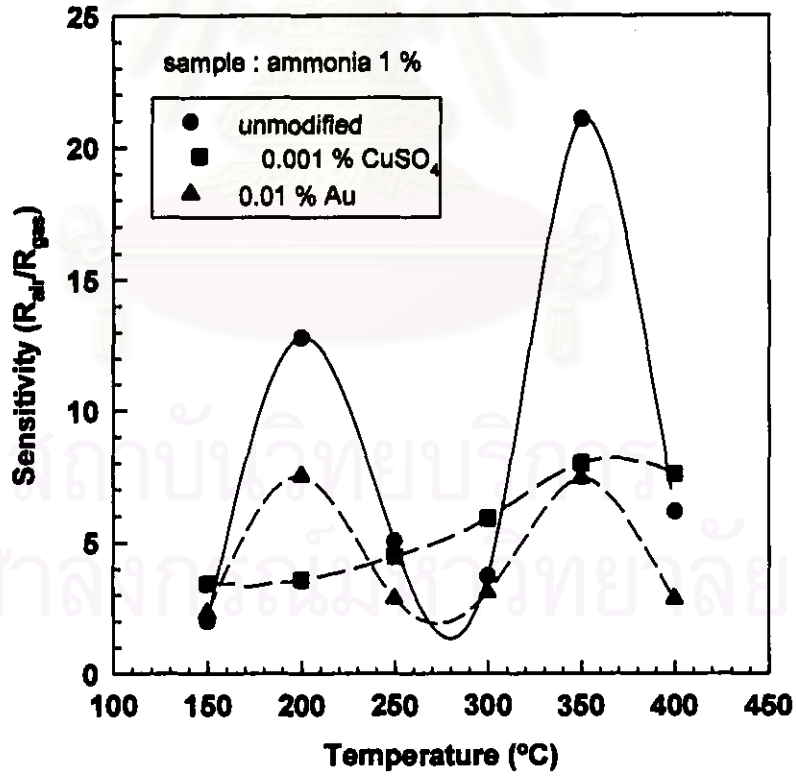

(b)

Fig. 6.23 Plot of Sensitivity against temperature of the unmodified SnO_2, $CuSO_4$-SnO_2 and Au-SnO_2 for (a) alcohol and (b) ammonia detection.

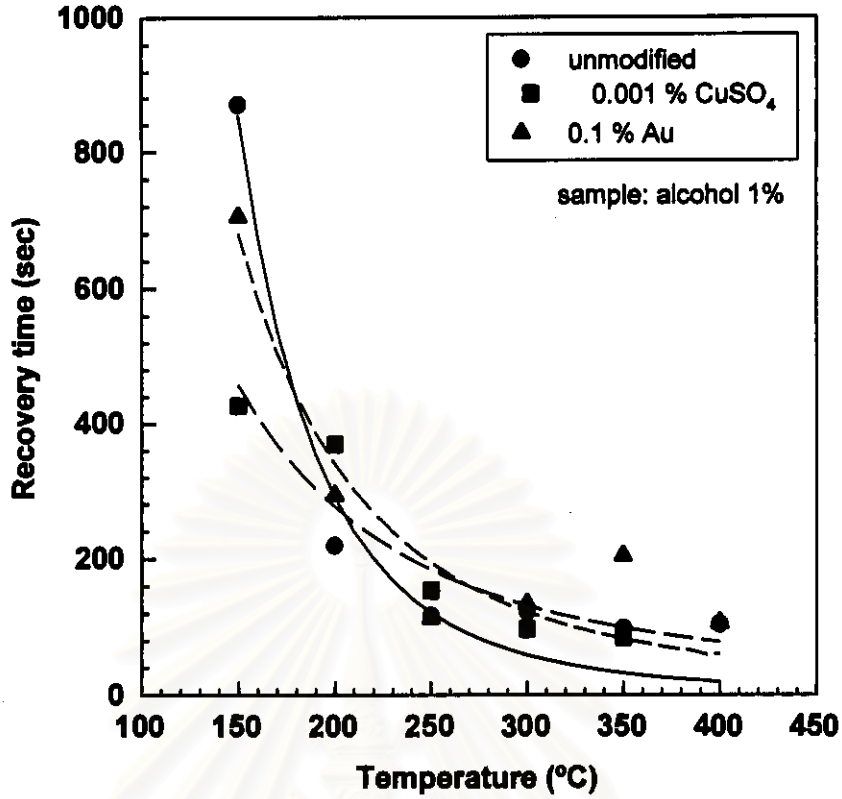

(a)

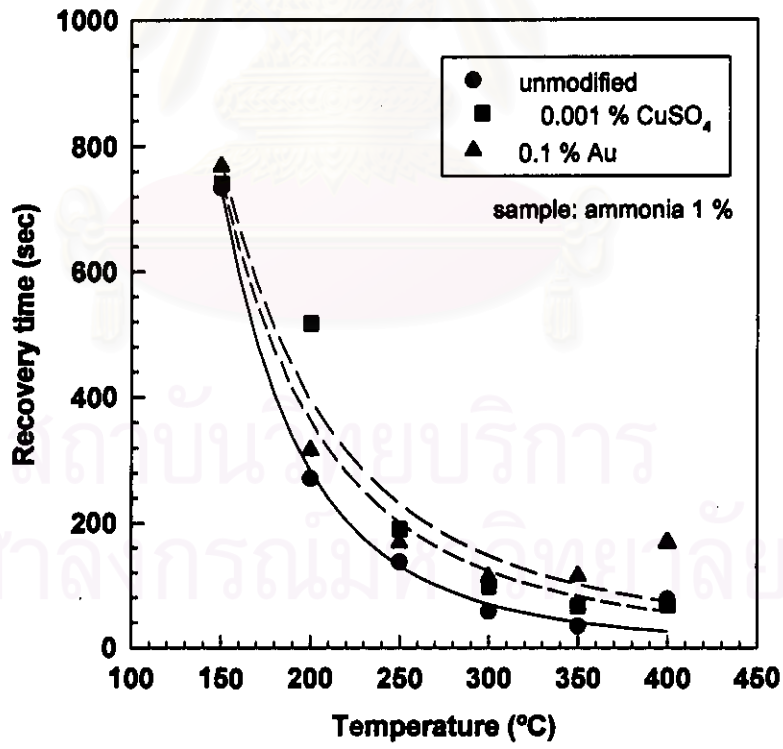

(b)

Fig. 6.24 Plots of recovery time of various SnO_2 gas sensors for the cases of (a) alcohol and (b) ammonia.

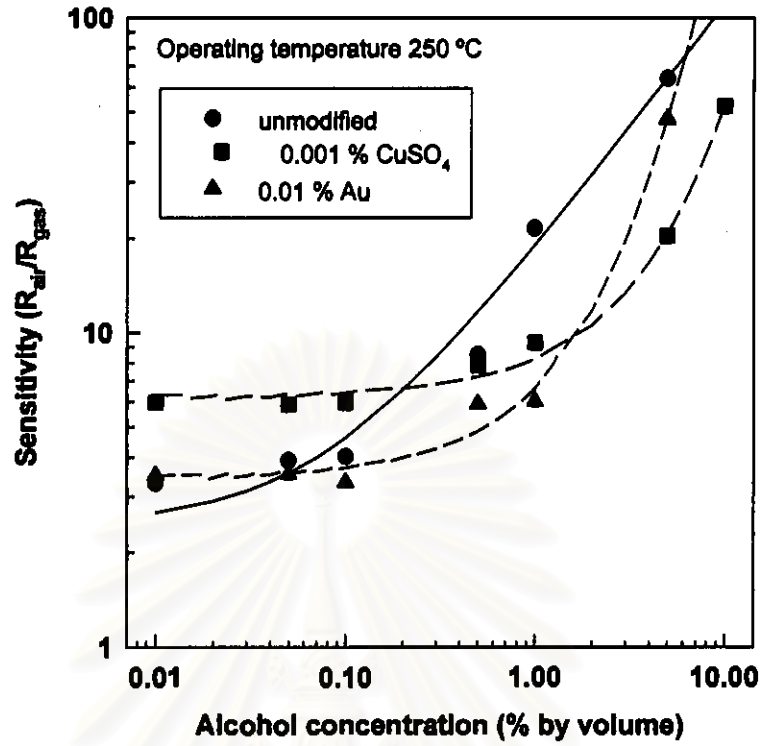

(a)

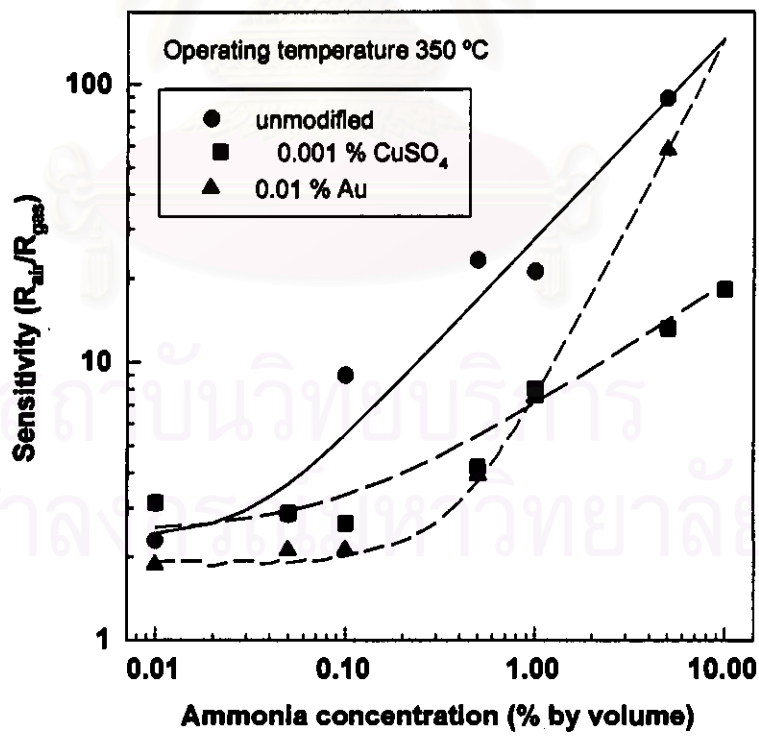

(b)

Fig. 6.25 Calibration curves of various SnO_2 gas sensors for (a) alcohol and ammonia.

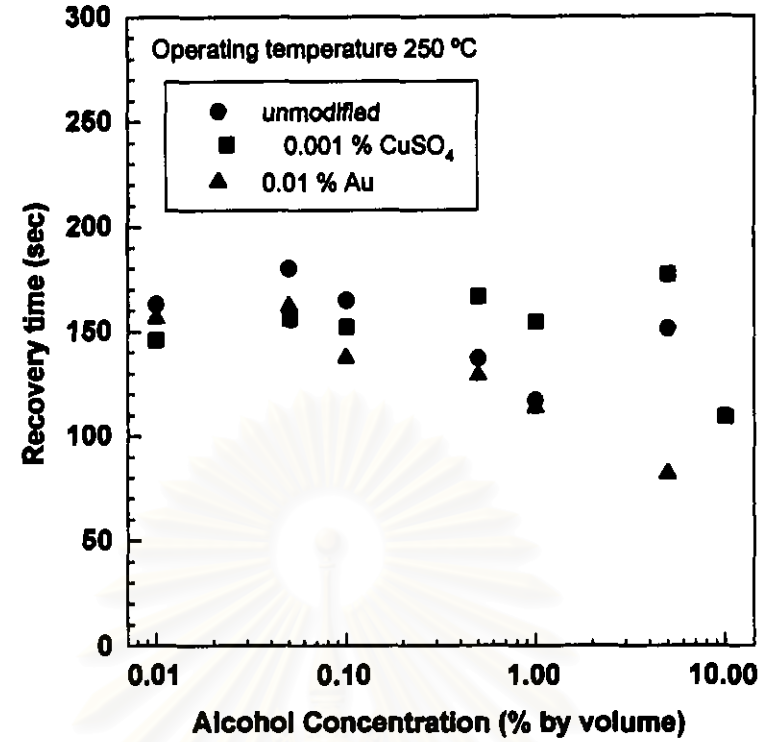

(a)

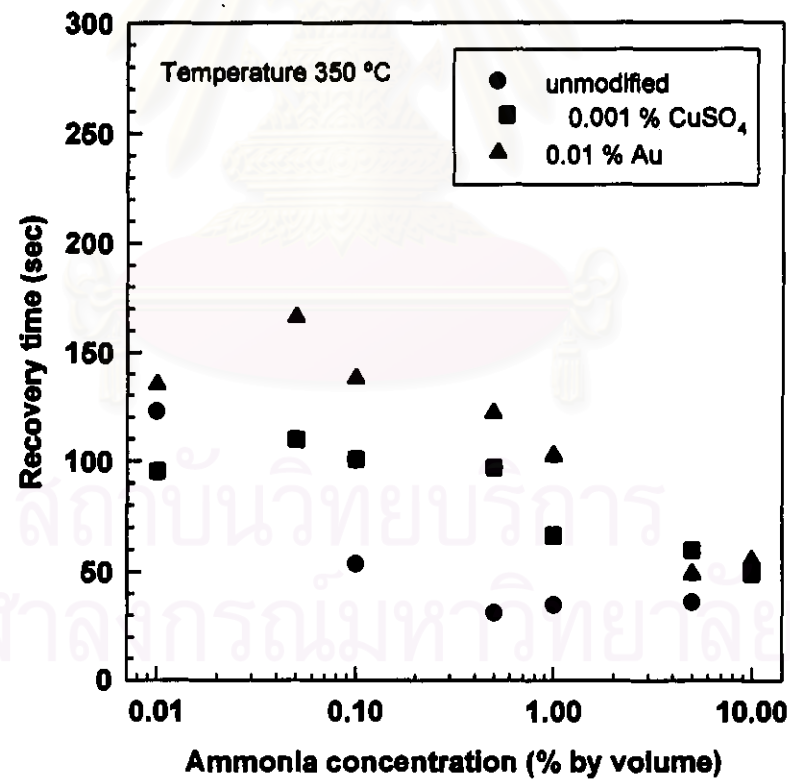

(b)

Fig. 6.26 Variation of recovery time of various SnO_2 gas sensors with sample concentration for (a) alcohol and ammonia.

The calibration curves of unmodified SnO_2, 0.001 % $CuSO_4$-SnO_2 and 0.01 % Au-SnO_2 sensor for alcohol at 250 °C and ammonia at 350 °C are given in Fig. 6.25. In Fig. 6.26 shows the variation of recovery time with sample concentration. Table 6.8 lists all parameters involving in power law model for various sensors. The lines are produced by fitting the measured values with the parameters in Table 6.8. The parameters fitted quite well with the measured data.

Table 6.8 Parameters involving in power law model for various SnO_2 sensors.

Sample	Sensor	a	k (1/k)	β
alcohol	unmodified	2.4276	12.5794 (0.08)	0.7885
	0.001 % $CuSO_4$	6.2977	0.5000 (2.00)	1.3270
	0.01 % Au	3.4848	0.8933 (1.12)	1.6876
ammonia	unmodified	2.7113	19.9725 (0.50)	0.7551
	0.001 % $CuSO_4$	2.4485	8.8326 (0.11)	0.4464
	0.01 % Au	1.7342	1.2837 (0.77)	1.7504

For the alcohol detection at 250 °C, the analysis results showed the $CuSO_4$-SnO_2 and Au-SnO_2 sensors gave higher detection limit than the unmodified SnO_2 sensor. The k values indicated that for alcohol detection, the unmodified SnO_2 sensors could detect the alcohol concentration from 0.08, to 10 % by volume. For ammonia detection, the unmodified SnO_2, $CuSO_4$-SnO_2 and Au-SnO_2 could detect the ammonia concentration from 0.05, 0.11 and 0.77 to 10 % by volume respectively. By considering at the detection limit (k values) and sensitivity coefficient (β values) of gas sensors we found that the unmodified SnO_2 gas sensor gave the best results. Moreover, the addition of modified substance reduced both of sensitivity and detection limit of gas sensors. In conclusion, the unmodified SnO_2 sensors exhibited the best results in both sensitivity and detection limit aspects.

6.4.3.2 $AgNO_3$-SnO_2 and $FeCl_3$-SnO_2 Sensors

The amount of $AgNO_3$ and $FeCl_3$ in SnO_2 films were set to the same value as in the case of $CuSO_4$ and Au modified SnO_2 sensors (0.001 - 1 % by weight). The variations of alcohol and ammonia sensitivity due to the additions of $AgNO_3$ and $FeCl_3$ at the operating temperature 350 °C are shown in Fig. 6.27. It was found that the addition of $AgNO_3$ had not much effect on the detection of alcohol and ammonia, (Fig. 6.27(a)), the gas sensitivity seemed to be nearly constant over the wide range of $AgNO_3$ concentration. In the case of $FeCl_3$, the gas sensitivity to ammonia increased with the amount of $FeCl_3$ in SnO_2 films, while, the sensitivity to alcohol slightly decreased. From these results, the amount of $AgNO_3$ and $FeCl_3$ in SnO_2 films that gave the highest sensitivity was 1 % by weight.

Fig. 6.28 contains the change of sensitivity of the unmodified SnO_2, $AgNO_3$-SnO_2 and $FeCl_3$-SnO_2 sensors versus the operating temperature. By considering the amplitude and peak position in Fig. 6.28, we found that the optimum temperature for alcohol detection was about 275 °C, this value was slightly different from that of the previous groups of sensors, the optimum temperature for ammonia detection was 350 °C. From these results, it is clear that the additions of $AgNO_3$ and $FeCl_3$ seemed to reduce the sensitivity to alcohol, however, the enhancement of ammonia detection could be achieved by the addition of $FeCl_3$. The plots of recovery time against the operating temperature of the unmodified SnO_2, $AgNO_3$-SnO_2 and $FeCl_3$ are given in Fig. 6.29. The recovery time of all sensors decreased significantly as temperature increased.

The calibration curve of the unmodified SnO_2, 1 % $AgNO_3$-SnO_2 and 1 % $FeCl_3$-SnO_2 for alcohol detection at 275 °C and for ammonia at 350 °C are given in Fig. 6.30. Table 6.9 contains all parameters involving in the power law model for various kinds of SnO_2 sensors. The lines in Fig. 6.30 are drawn by fitting the measured values with the parameters in Table 6.9. The change of recovery time against alcohol and ammonia concentration are shown in Fig. 6.31.

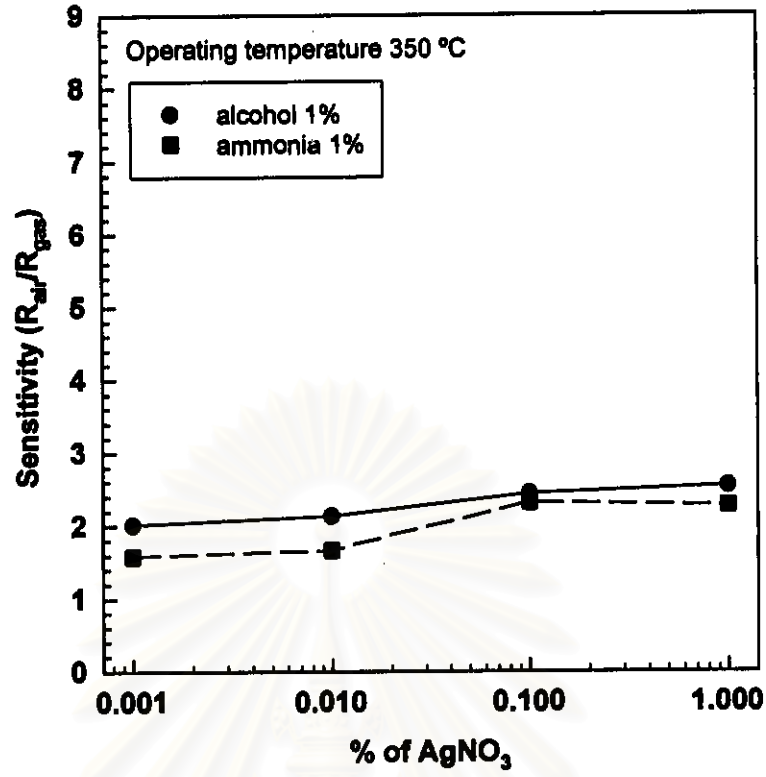

(a)

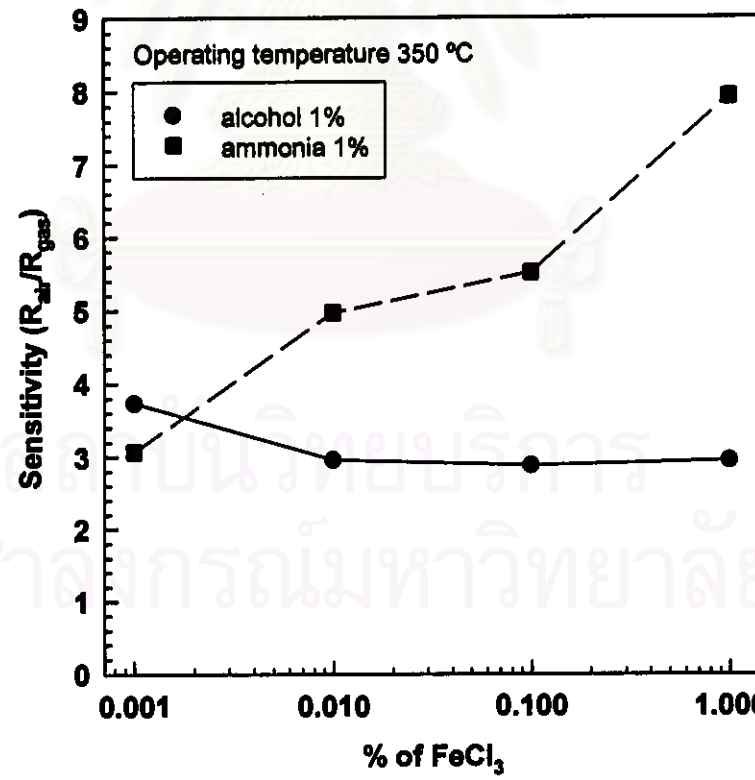

(b)

Fig. 6.27 Variation of gas sensitivity as a function of (a) $AgNO_3$ and (b) $FeCl_3$

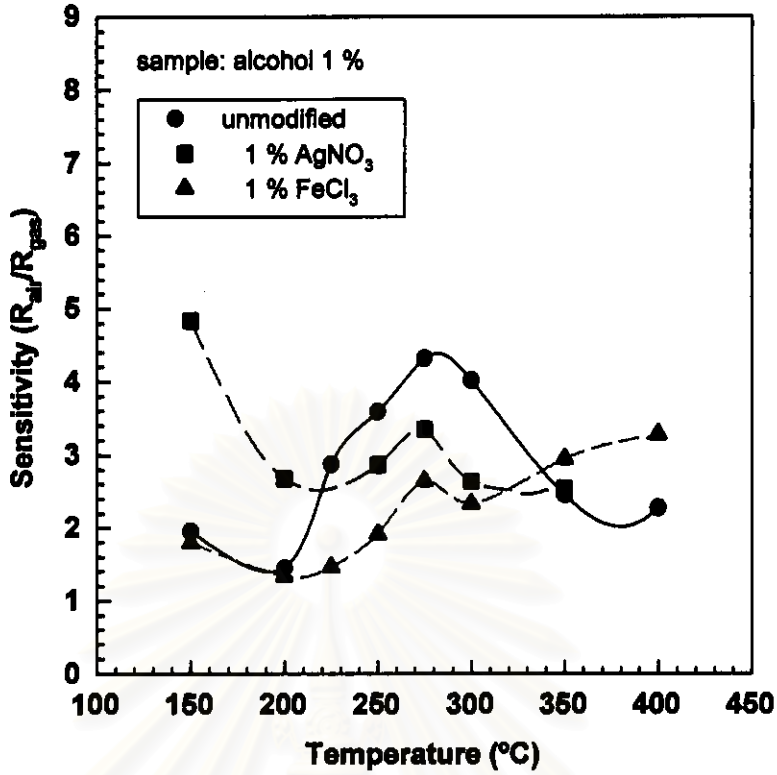

(a)

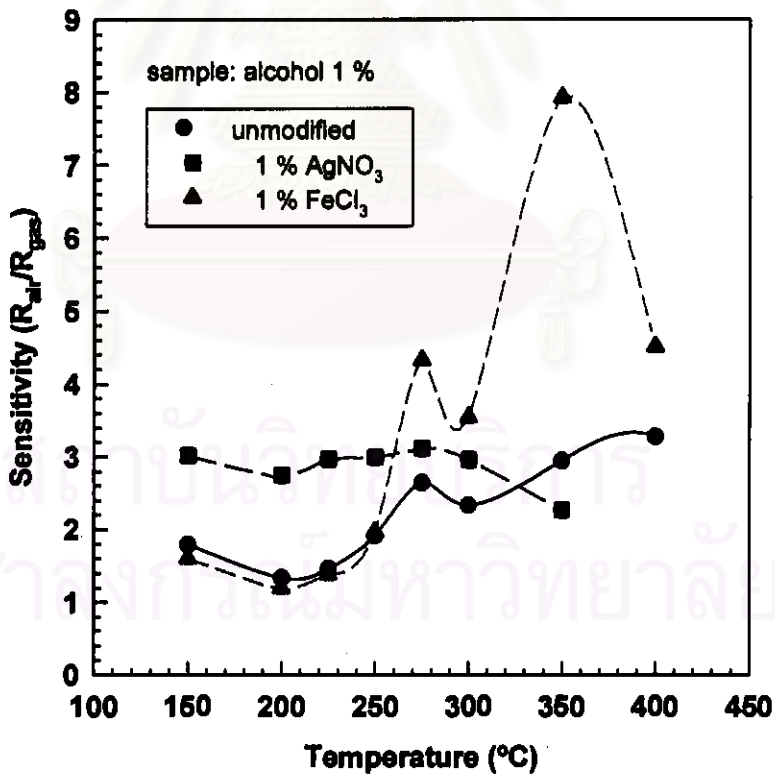

(b)

Fig. 6.28 Plots of gas sensitivity versus temperature of various SnO_2 sensors: for (a) alcohol and (b) ammonia.

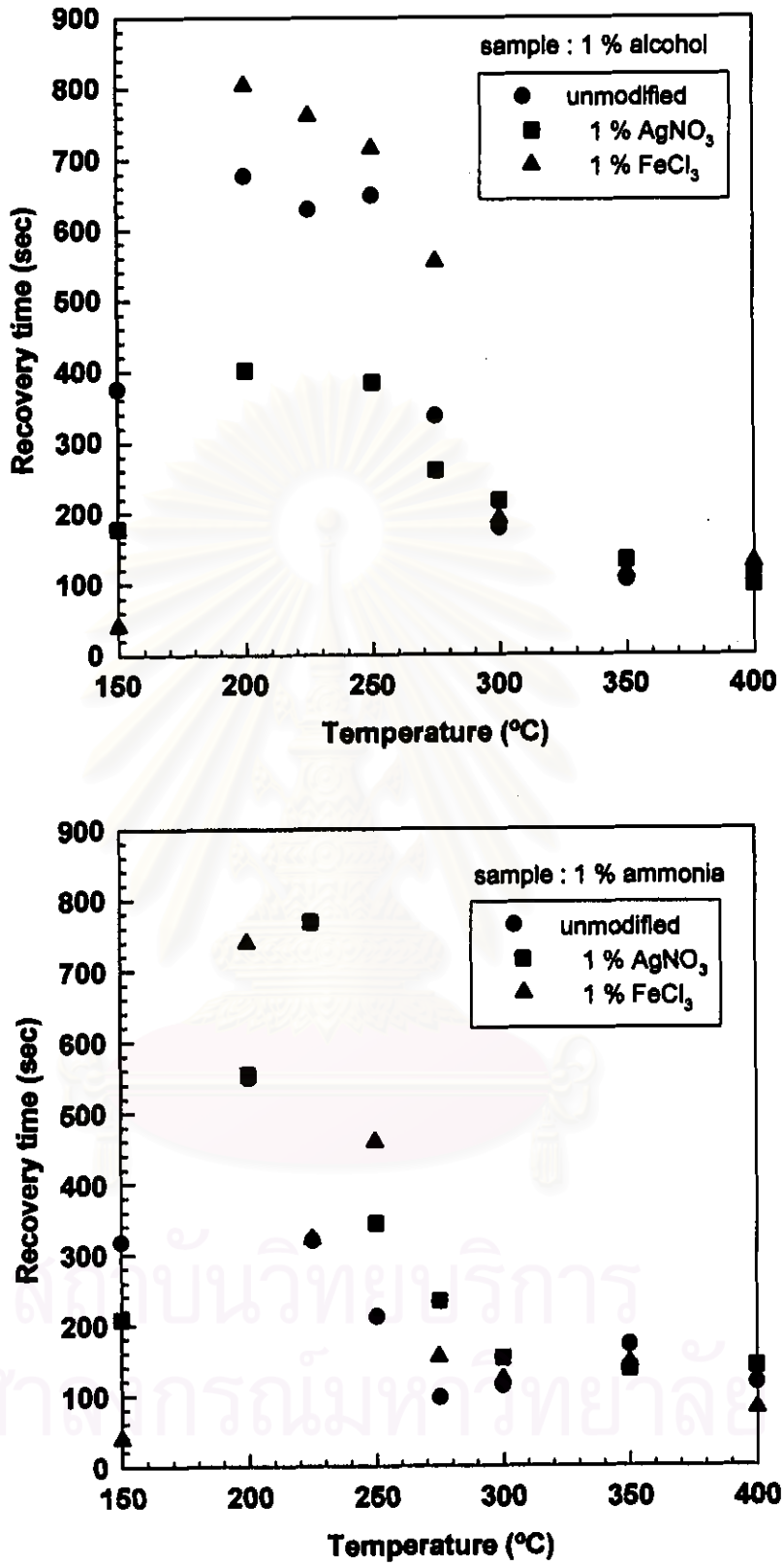

Fig. 6.29 The relation between recovery time and temperature of the unmodified SnO_2, $AgNO_3$-SnO_2 and $FeCl_3$-SnO_2 for (a) alcohol and (b) ammonia.

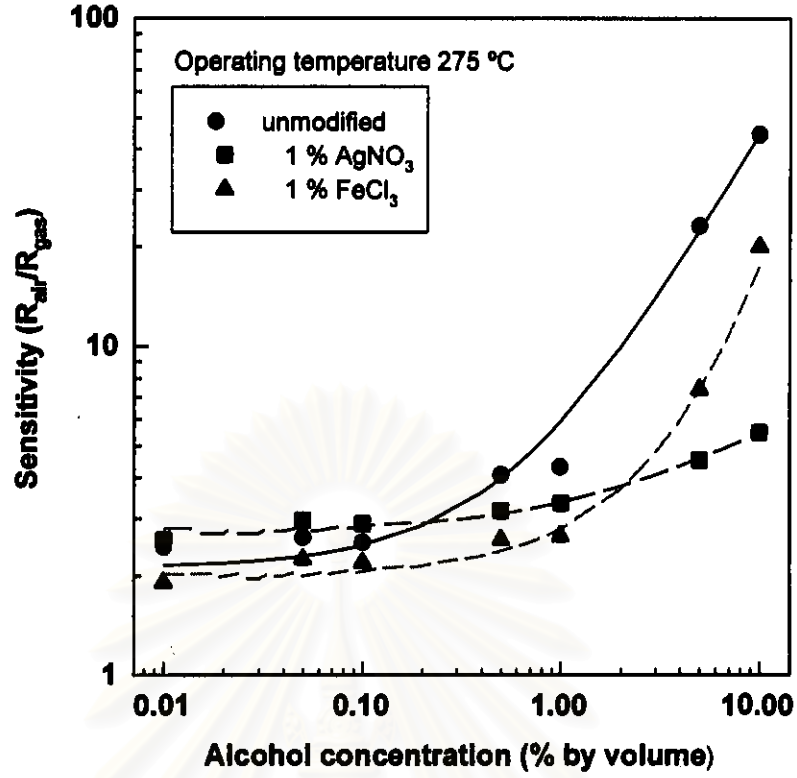

(a)

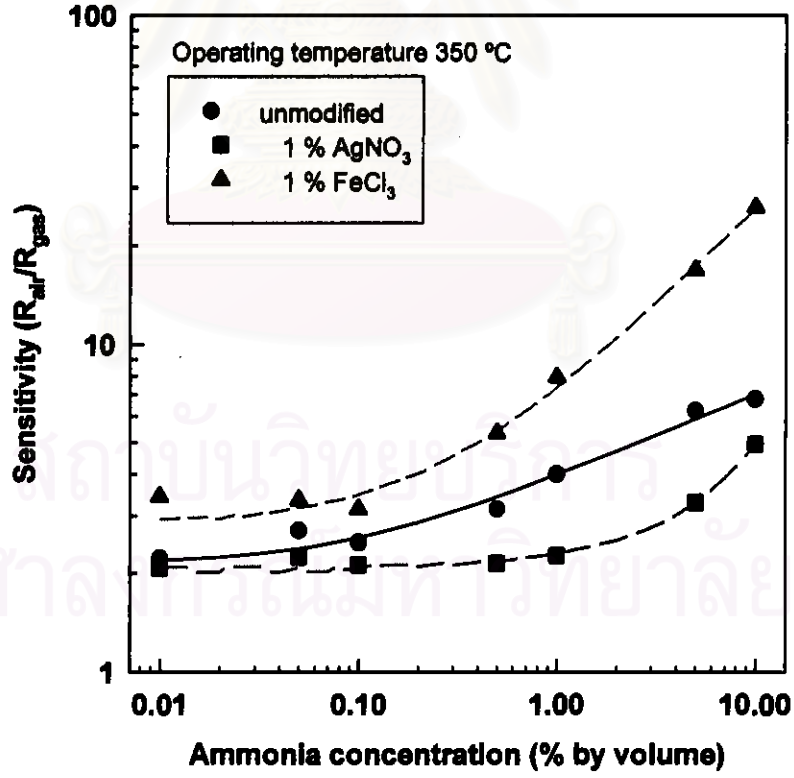

(b)

Fig. 6.30 Calibration curves of various SnO_2 gas sensors: unmodified, $AgNO_3$-SnO_2 and $FeCl_3$-SnO_2 for (a) alcohol and (b) ammonia.

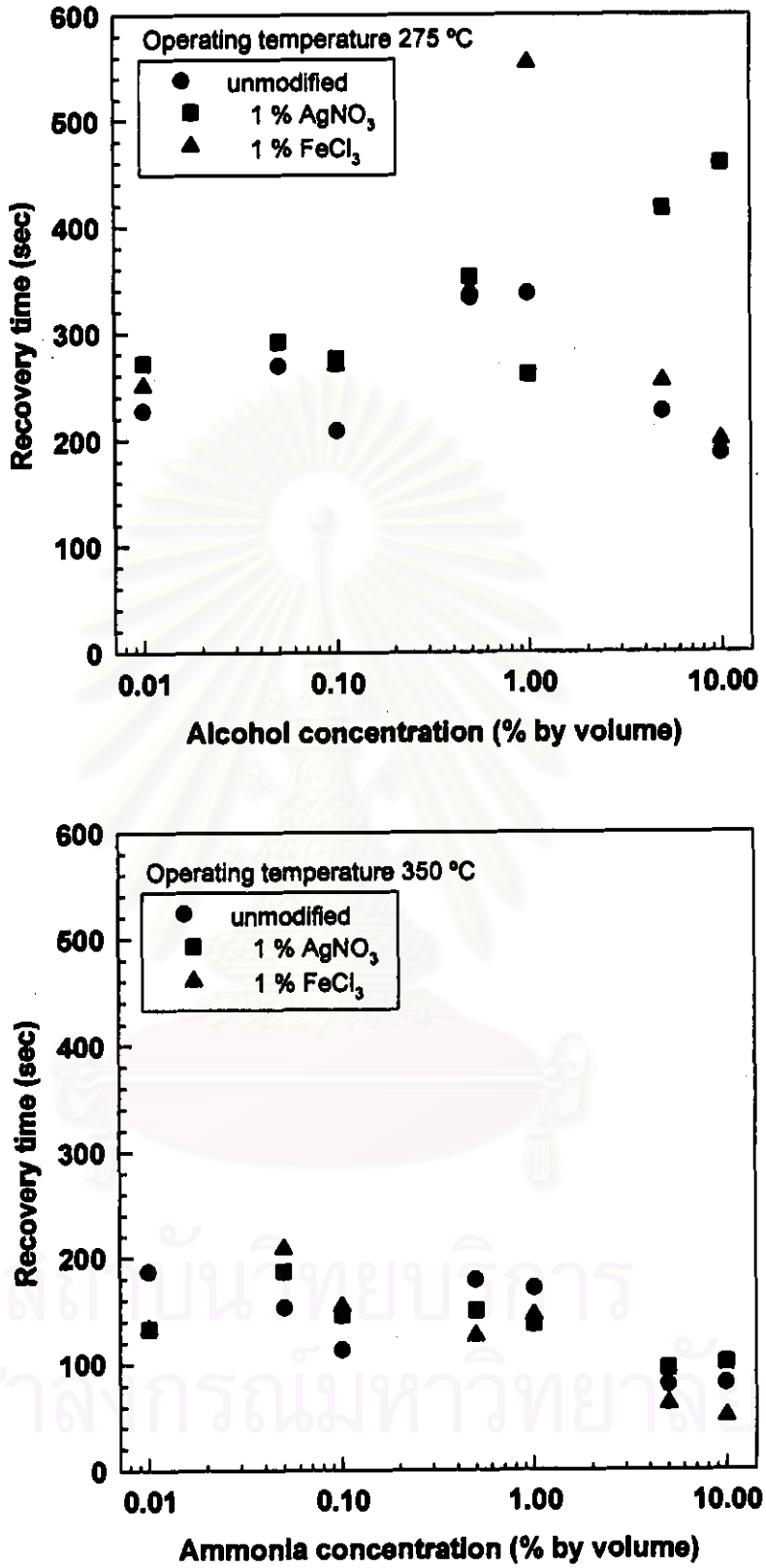

Fig. 6.31 The relation between recovery time and sample concentration of the unmodified SnO_2, $AgNO_3$-SnO_2 and $FeCl_3$-SnO_2 for (a) alcohol and (b) ammonia.

Table 6.9 Parameters involving in power law model for various SnO_2 gas sensors.

Sample	Sensor	*a*	*k (1/k)*	*β*
alcohol	unmodified	2.1283	1.5810 (0.63)	1.0782
	1 % $AgNO_3$	2.7912	0.8820 (1.13)	0.2927
	1 % $FeCl_3$	2.0301	0.4788 (2.01)	1.4709
ammonia	unmodified	2.1367	10.8982 (0.09)	0.2532
	1 % $AgNO_3$	2.0928	0.3845 (2.60)	0.6803
	1 % $FeCl_3$	2.8597	3.8357 (0.26)	0.5996

According to the above table, the addition of $AgNO_3$ and $FeCl_3$ into the parent SnO_2 reduced the sensitivity to alcohol and also the detection limit (determining from the *k* values). The *k* values indicated that for alcohol detection, the unmodified SnO_2 sensors, could detect alcohol concentration from 0.6 to 10 % by volume. For ammonia detection, the addition of $FeCl_3$ enhanced the gas sensitivity, however, it also reduced the detection limit about two times. While, $AgNO_3$ gave the lowest sensitivity and the higher detection limit. The unmodified SnO_2 and $FeCl_3$-SnO_2 could detect ammonia concentration from 0.09 and 0.26 to 10 % by volume respectively. In conclusion, the addition of $FeCl_3$ showed a possibility to enhance the detection of ammonia.

By comparing two groups of sensors in the section 6.4.3.1 and 6.4.3.2, we found that in the overview picture, the sensors in the section 6.4.3.2 had lower sensitivity than the sensors in the section 6.4.3.1. This may result from the aging of the starting precursor, since the metal alkoxide suffers from the slow gelation process due to the absorption of water molecule from the surrounding ambient. This process has the effect on the increase of grain size, therefore, it results in the decrease of sensitivity.

Fig. 6.29 shows the variation of recovery time with the operating temperature of gas sensors. It was clear that all gas sensors exhibited a decrease of recovery time with the operating temperature. Since, the rate of reaction that a gas desorps from a semiconductor surface, increase with temperatures. However, the variation of recovery time with gas concentration seemed to be complicated, since, the test samples are the mixtures between H_2O and alcohol or ammonia. The recovery time depended on the desorption rate of both water molecules and gas molecules from SnO_2 surface. However, in most cases, the recovery time seemed to decrease with sample concentrations.

Table 6.9 summarized the results obtained from the power law model on the SnO_2 gas sensors prepared from various sol solutions. In each cell of this table contains two symbols separating by a slash "/". The first symbol means detection limit and the second symbol means sensitivity. For the rigorously controlled sol, the unmodified SnO_2 sensors have two set of data, the first one represents data from the freshly prepared sol and the second one represents the data from the aging sol. The other explanations are shown under the Table. According to the table, it was found that the SnO_2 gas sensors fabricated from the rigorously controlled sol gave the best results in the sensitivity in both alcohol and ammonia detection. However, from the detection limit point of view, SnO_2 gas sensors prepared from the commercial sol gave the best detection limit for alcohol detection, while, SnO_2 gas sensors from the rigorously controlled sol gave the best detection limit for ammonia detection.. Moreover, the SnO_2 gas sensors fabricated from this sol also gave the fastest recovery time (Fig. 6.26 and Fig. 6.29).

Table 6.10 Summary of SnO_2 sensors prepared from various sols.

Alcohol detection					
Sol Solution	**Sensors**				
	Unmodified	**$AgNO_3$**	**$FeCl_3$**	**Au**	**$CuSO_4$**
Commercial	O/×	O/×	O/Δ	O/Δ	-
Mixed	O/×	-	-	-	O/Δ
Controlled	O/O(Δ/O)	×/×	×/O	×/O	×/O

Ammonia detection					
Sol Solutions	**Sensors**				
	Unmodified	**$AgNO_3$**	**$FeCl_3$**	**Au**	**$CuSO_4$**
Commercial	Δ/Δ	×/×	×/Δ	Δ/Δ	-
Mixed	×/Δ	-	-	-	×/Δ
Controlled	O/O(O/Δ)	×/×	Δ/O	Δ/O	Δ/Δ

Commercial : the commercial sol Mixed : the simple mixed sol

Controlled : the rigorously controlled sol

O : good, Δ : fair and × : poor

6.5 Summary

In this chapter, the characterizations of gas sensing performance of the fabricated gas sensors are described. We adopted the modified power law model to compare the performance of gas sensors in more quantitative ways. We found that the developed SnO_2 gas sensor, prepared from the rigorously controlled sol, gave the highest sensitivity and the fastest detection for alcohol and ammonia. The aging time of the sol was one of the important parameter to determine the sensing performance of gas sensors. The best results were obtained from the unmodified SnO_2 gas sensors prepared from the freshly synthesized sol. These sensors could detect alcohol and

ammonia ranging from 0.08-10 % and 0.05 and 10 % respectively. However, there was a trend to enhance gas sensitivity to ammonia detection by corporation of $FeCl_3$. The developed sensors shows the potential applications in the field of biotechnology which engages with the concentration ranging from 0.1-10 % by volume.